MECHANISTIC STUDIES OF THE ELECTRODEPOSITION OF POLYTHIOPHENES

ZIWEI ZHAO

MECHANISTIC STUDIES OF THE ELECTRODEPOSITION OF POLYTHIOPHENES

by
Ziwei Zhao

A thesis submitted to the

School of Graduate Studies

in partial fulfilment of the

requirements for the degree of

Master of Science

Department of Chemistry
Memorial University of Newfoundland

July 1993

St. John's Newfoundland

ISBN 0-315-86623-3

Canada

To my parents and my husband

Abstract

The electrochemical deposition of poly(3-methylthiophene) and the electrochemical polymerization of 3-bromothiophene in the presence of 2,2'-bithiophene have been studied. Mechanisms have been proposed, based on the electrochemical responses recorded during polymer formation and characterization of the resulting polymer films by cyclic voltammetry, ac impedance spectroscopy, scanning electron microscopy as well as by x-ray emission spectroscopy.

A rotating Pt disc electrode was applied to probe the potentiostatic deposition of poly(3-methylthiophene). It was observed that poly(3-methylthiophene) films could be formed on both stationary and rotating electrodes even at rotation rates as high as 1600 rpm (revolutions per minute), and that the quantity of polymer deposited decreased with increasing rotation rate. It was therefore concluded that polymer deposition takes place both through the precipitation of oligomeric intermediates from the solution, and via the coupling of monomeric species with polymer chain ends in the polymer film matrix. Chronoamperometric responses recorded during polymerization, as well as the characterization of the resulting polymer films by cyclic voltammetry, ac

impedance spectroscopy and scanning electron microscopy, demonstrated that the deposition of oligomeric intermediates from the solution contributes most to polymer formation on a stationary electrode. On the other hand, polymer growth on a rapidly rotating electrode occurs primarily by the incorporation of monomeric species into polymer chains grafted on the electrode surface. Much smoother, more homogeneous films were deposited on rotating electrodes.

The polymerization of 3-bromothiophene in the presence of 2,2'-bithiophene was investigated by cyclic voltammetry. With a catalytic amount of 2,2'-bithiophene, a significant increase in the polymerization rate, together with a decrease in the potential required for poly(3-bromothiophene) formation, was observed. The polymer coated electrodes from the mixed solution exhibited characteristic electrochemical behaviour in cyclic voltammograms and Br and S peaks in x-ray emission spectroscopy for pure poly(3-bromothiophene). The 2,2'-bithiophene catalyst produces better quality poly(3-bromothiophene) films. A polymerization mechanism involving radical-monomer coupling is supported by these experimental observations. In this mechanism, the 2,2'-bithiophene catalyst is oxidized first, and then couples with 3-bromothiophene to initiate the polymerization.

TABLE OF CONTENTS

List of Figures

List of Tables

Acknowledgement

I wish to express my sincere gratitude to my supervisor, Dr. Peter G. Pickup for his inspiring supervision and patient guidance throughout the course of the degree programme.

I would like to thank Ms. Carolyn Emerson for her help in operating the scanning electron microscope and x-ray emission spectroscope.

Financial support of the Department of Chemistry and supplements from an NSERC grant are gratefully acknowledged.

Chapter 1

The Electrochemical Polymerization of Pyrroles and Thiophenes

1.1 General Aspects

Conducting polymers prepared by the electrochemical polymerization of heterocyclic monomers have been the subject of much work over the last 15 years, due to their prosperous technical applications such as rechargeable battery electrodes, electrochromic displays, substrates for metal deposition and sensors.[1-8] Since the first electrodeposition reported by Dall'Olio and co-workers for producing a conducting polypyrrole black in aqueous sulphuric acid,[9] there has been great interest in the electrochemical polymerization of aromatic compounds, such as pyrrole,[10,11] and thiophene.[12,13]

The electrodeposition reaction proceeds with electrochemical stoichiometry. It has been observed that besides the 2 electrons per molecule of monomer required

for the polymerization, an excess of charge is consumed owing to the oxidation or doping of the resulting polymer. As the potential applied is always significantly higher than the oxidation potential of the resulting polymer, both polymer film growth and its oxidation occur simultaneously. Therefore, n values (*i.e.*, the total charge consumed in the polymerization process) in the range of 2.1-2.5 Faradays/mol have been commonly measured,[14-16] depending on the electrolyte anion used and the reaction conditions.[17] That is, the polymer generated carries 0.1 to 0.5 oxidized centres per monomer unit, balanced by the incorporated electrolyte anion. The electrodeposition process is not generally diffusion limited, as evidenced by the linear relationship of the absorbance of the resulting polymer with reaction time,[17,18] and the decrease of the current function $I_p/v^{1/2}$ accompanying the polymerization process during cyclic voltammetry.[19]

The polymerization reaction takes place primarily through linkage at the α-positions (*i.e.*, 2- and 5- positions) of the monomer, β- coupling (*i.e.*, linkage at the 3- or 4- positions) being less important, as evidenced by the fact that no polymer formation occurs with α- substituted monomers,[15] and confirmed by IR and NMR studies.[20,21] However, the proportion of β-position linkages has been demonstrated to increase with the polymeric chain growth.[14] In order to increase the regularity

and the extent of conjugation of the polymer backbone, which may result in improved conductivity and magnetic properties, approaches to increase the number of α,α-linkages in the polymer chain have been made, such as using a dimer or higher oligomer as the starting material,[21-23] or using β- substituted monomers for the polymerization.[24] However, studies have shown that polymers prepared from dimeric or higher oligomeric species were different from those obtained via polymerization of the monomer in terms of electrochemical behaviour and optical properties.[21,22]

Electrochemically generated polymer films generally exhibit useful electrical, electrochemical and other properties. These electroactive polymer films can be switched repetitively between the neutral (nonconducting) and the oxidized (conducting) states.[25-27] In general, the charge consumed for film doping or oxidation lies between 0.25 and 0.4 Faraday/mol, indicating that every three or four monomeric units in the film carry one positive charge.[15] The electrochemical behaviour depends greatly on the nature of the ions compensating the cationic sites in the film.[15] However in all cases, taking a polymer film to a too positive potential leads to nucleophilic attack by water or the anion on the polymeric species, a loss of polymer chain conjugation, and loss of conductivity.[28-30]

Although polypyrrole is probably the most studied material in this field, in recent reports polythiophene in particular has received a great deal of attention, due to the fact that both its doped and undoped states are highly environmentally stable, and that its β- derivatives are more easily synthesized and produce polymers with less mislinkages and cross-linking.[30,31]

1.2 Mechanisms of Electropolymerization

In recent years, there have been a growing number of investigations of the mechanism of electropolymerization of heterocyclic monomers. Many techniques have been applied to these investigations, such as cyclic voltammetry,[19,32-37] chronoamperometry,[19,22,38-40] chronocoulometry,[17,21,23] the electrochemical quartz crystal microbalance,[18,41,42] ellipsometry[24] and optical absorption techniques.[17,43] Despite these efforts to elucidate the mechanism of electrochemical polymerization, the initial deposition step and the subsequent growth of polymer chains are still far from a full understanding. However, it is certain that the first step in electropolymerization is the formation of a radical cation by the oxidation of the monomer.[36] The resulting monomeric radical cations in the vicinity of the electrode have been detected by

ultrafast cyclic voltammetry.[44]

It is accepted that polymer chain propagation occurs by a radical-radical coupling process (r-r)[17,42] or by a radical-monomer coupling process (r-m).[39,45] The deposition of polymer on the electrode surface is thought to take place either by the precipitation of oligomeric intermediates from the solution (sol.)[11,35,46] or by the incorporation of monomeric species into the polymer matrix (surf.).[21,47] In the literature, much work has been done to elucidate which of these various mechanisms occur but many conflicting conclusions have been drawn. Table 1.1 lists some of the references and the polymerization analyzed, the methods used and the mechanisms proposed, *etc*. It is clear that the mechanism of electropolymerization is still not well understood.

1.2.1 Radical-Radical (r-r) Coupling Mechanism

A mechanism involving radical cation coupling for the polymer chain propagation was first proposed by Diaz and co-workers.[15,17] As illustrated in Scheme 1.1 for the polymerization of thiophenes by this mechanism, the first step is the oxidation of the monomer to its radical cation. The radical cations then dimerize

Table 1.1 Survey of the literature on the electrochemical polymerization of pyrroles and thiophenes

Year	Monomer	Electrode Substrate	Solvent	Electrolyte	Techniques	Mechanisms	Ref. No.
1983	Py	IO	CH_3CN	$LiClO_4$	Chronoabs. CV Chronoamp.	r-r	17
1984	Py	Pt	H_2O CH_3CN	KNO_3 Et_4NBF_4	CV Chronoamp.	r-m	19
1984	Py				MO	r-r	14
1986	Th, BiTh	Pt	CH_3CN	Bu_4NBF_4	Chronoamp. CV	nucleation	22
1986	Py	Pt	H_2O/CH_3CN	Bu_4NBF_4	CV Chronoamp.	nucleation	56
1987	Th	Au	CH_3CN	Et_4NBF_4	Chronoamp.	nucleation	40
1987	Py	Pt	H_2O	H_2SO_4	CV	r-m	37
1988	Th	Pt	CH_3CN	Bu_4NClO_4	CV, RRDE	r-r, sol.	34
1988	MeTh	Pt	CH_3CN	$LiClO_4$	Ellip., CV RDE	surf.	24
1988	Py	Au	CH_3CN	Bu_4NBF_4 *etc.*	EQCM	r-r, sol. surf.	18

Table 1.1 contd.

1988	Th	Pt	CH_3CN	Bu_4NBF_4	FTIR	monomer ads.	57
1989	Py	Pt	H_2O	KNO_3 *etc.*	Ellip. Chronoamp. FTIR	nucleation	63
1990	Py	C. Pt	CH_3CN	$NaClO_4$	CV, RRDE	sol.	35
1990	Py	Pt	H_2O/CH_3CN	Bu_4NBF_4 *etc.*	RDE, RRDE CV	r-r	36
1990	MeTh	Au	CH_3CN	$LiClO_4$	EQCM, CV	sol.	64
1991	Th	Pt	CH_3CN	$LiClO_4$	RDE, CV Chronoamp.	surf.	32
1991	Py	Pt	CH_3CN H_2O	Bu_4NClO_4 NaCl	CV Chronoamp.	sol.	33
1991	Py	C. Au	H_2O	KNO_3	Chronoamp.	r-m, sol	38
1991	MeTh Th. *etc.*	Pt	CH_3CN	$LiClO_4$	CV, IR, SEM	r-m	45
1992	MeTh	ITO	CH_3CN	Bu_4NPF_6	Optical Microscopy	sol. nucleation	46

Table 1.1 ccontd.

1992	Th-3-acetic acid	Pt	CH_3CN	$LiClO_4$	Chronoamp.	r-r 2D nucleation	54
1992	Py	Au	H_2O CH_3CN	NaCl $LiClO_4$	EQCM. CV	r-r	42

List of abbreviations in Table 1.1:

Monomer:

Py: pyrrole
Th: thiophene
Bith: 2,2-bithiophene
MeTh: 3-methylthiophene

Electrode:

Pt: platinum electrode
Au: gold electrode
IO: indium oxide optically transparent electrode
C: vitreous carbon electrode
ITO: indium-tin oxide

Techniques:

CV: cyclic voltammetry
Chronoamp.: chronoamperometry
Chronoabs.: chronoabsorptometry
MO: molecular orbital method
Ellip.: ellipsometry
EQCM: electrochemical quartz crystal microbalance
FTIR: Fourier transformation infra-red spectroscopy
SEM: scanning electron microscopy
RDE: rotating disc electrode
RRDE: rotating-ring disc electrode

Mechanism:

r-r: radical-radical coupling
r-m: radical-monomer coupling
sol.: polymerization in the solution
surf.: polymerization on the electrode surface
2D: two-dimensional (nucleation)
ads.: adsorption

SCHEME 1.1

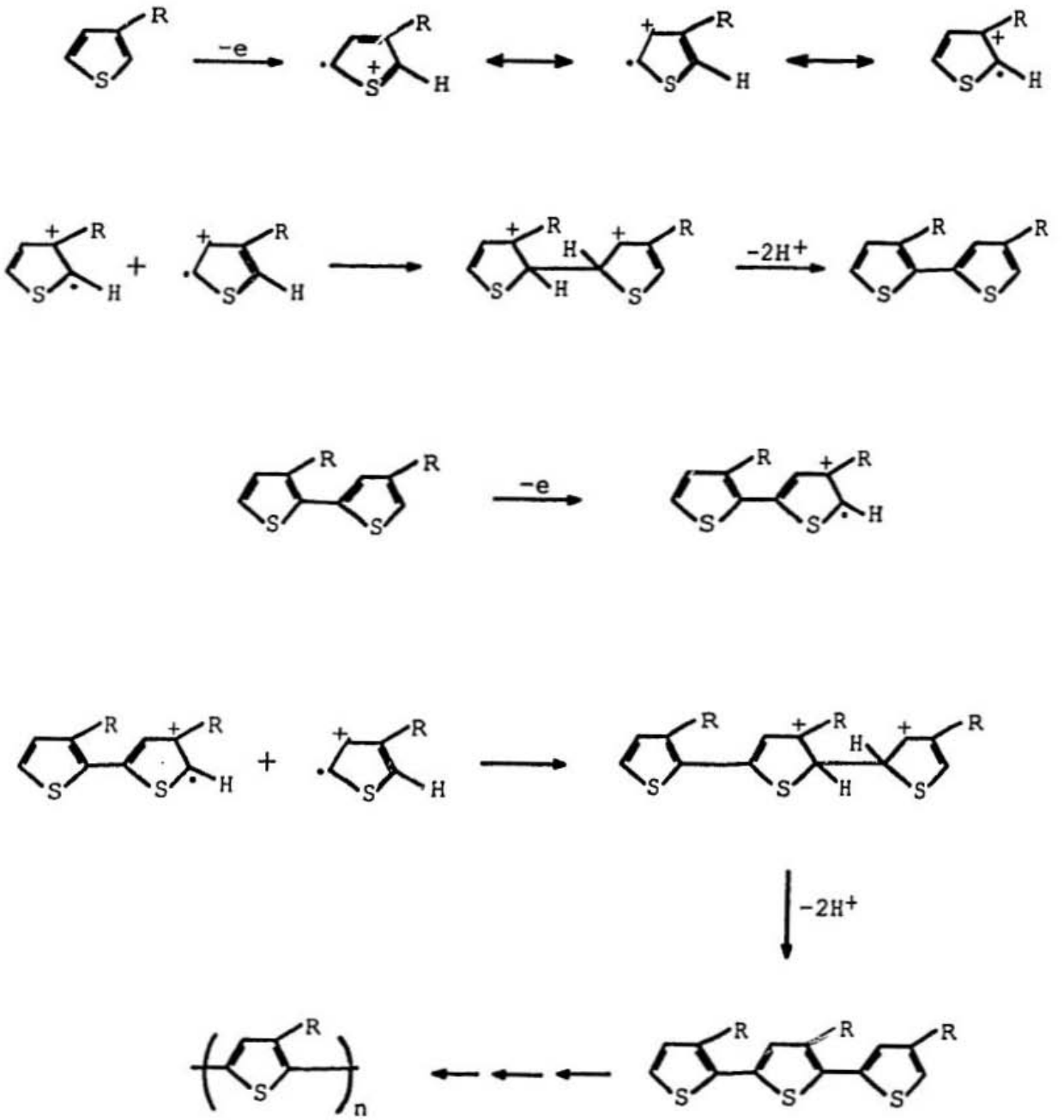

to produce a dimeric dihydro dication, from which a dimer is generated after deprotonation. Since the dimer and higher oligomers are more readily oxidized than the monomer,[47] further polymerization can involve the coupling of oligomeric radical cations with each other or with monomeric radical cations.[47-49] The oligomer intermediates eventually become insoluble in the synthesis solution, and precipitate onto the electrode surface, forming a conducting polymer film.

This mechanism has been favoured by most authors, based on general considerations,[17,27] specific studies,[36,50] and MO calculations.[14,36,51] It was supported by the observation that an applied polymerization potential high enough for the oxidation of monomer, not the dimer or oligomers was required through-out the polymerization of pyrrole.[17,47] In addition, investigations of the copolymerization of pyrrole with substituted pyrroles showed that a copolymer could not be generated at potentials where only one of the monomers was oxidized.[18,41] Studies on the electrochemical dimerization of diphenylpyrazoline produced similar experimental observations and were successfully interpreted by this mechanism.[52] However, conducting copolymer films of pyrrole and $[Ru(bp)_2(pmp)Cl]^+$ (bp=2,2'-bipyridine, pmp=3-(pyrrole-1-methyl)pyridine) have been synthesized at potentials where the oxidation of $[Ru(bp)_2(pmp)Cl]^+$ in the absence of pyrrole does not occur.[53]

In the r-r mechanism, the radical-coupling step was suggested to be rate-determining,[17] as supported by microgravimetric studies where the deposition rates determined from mass-time slopes were found to be proportional to the second order of the pyrrole monomer concentration,[18] and by the modified MO model.[36] However, this direct dimerization has been questioned by some authors,[19] since it will be hindered by the strong coulombic repulsion between the small cation radicals. In addition, some authors suggested that the oxidation of the monomer is the rate determining step of the polymerization.[38,45,54]

1.2.2 Radical-Monomer (r-m) Coupling Mechanism

The so-called radical-monomer coupling mechanism was postulated by Pletcher et al.,[19] in an attempt to account for their experimental observations of polypyrrole deposition. Marcos et al.[17] supported this hypothesis and proposed the coupling of an adsorbed radical cation with a neighbouring adsorbed monomer as the initiation step for the subsequent polymerization.

Scheme 1.2 illustrates the proposed radical-monomer coupling mechanism (without absorption) for the electrosynthesis of thiophenes, where the first step is

SCHEME 1.2

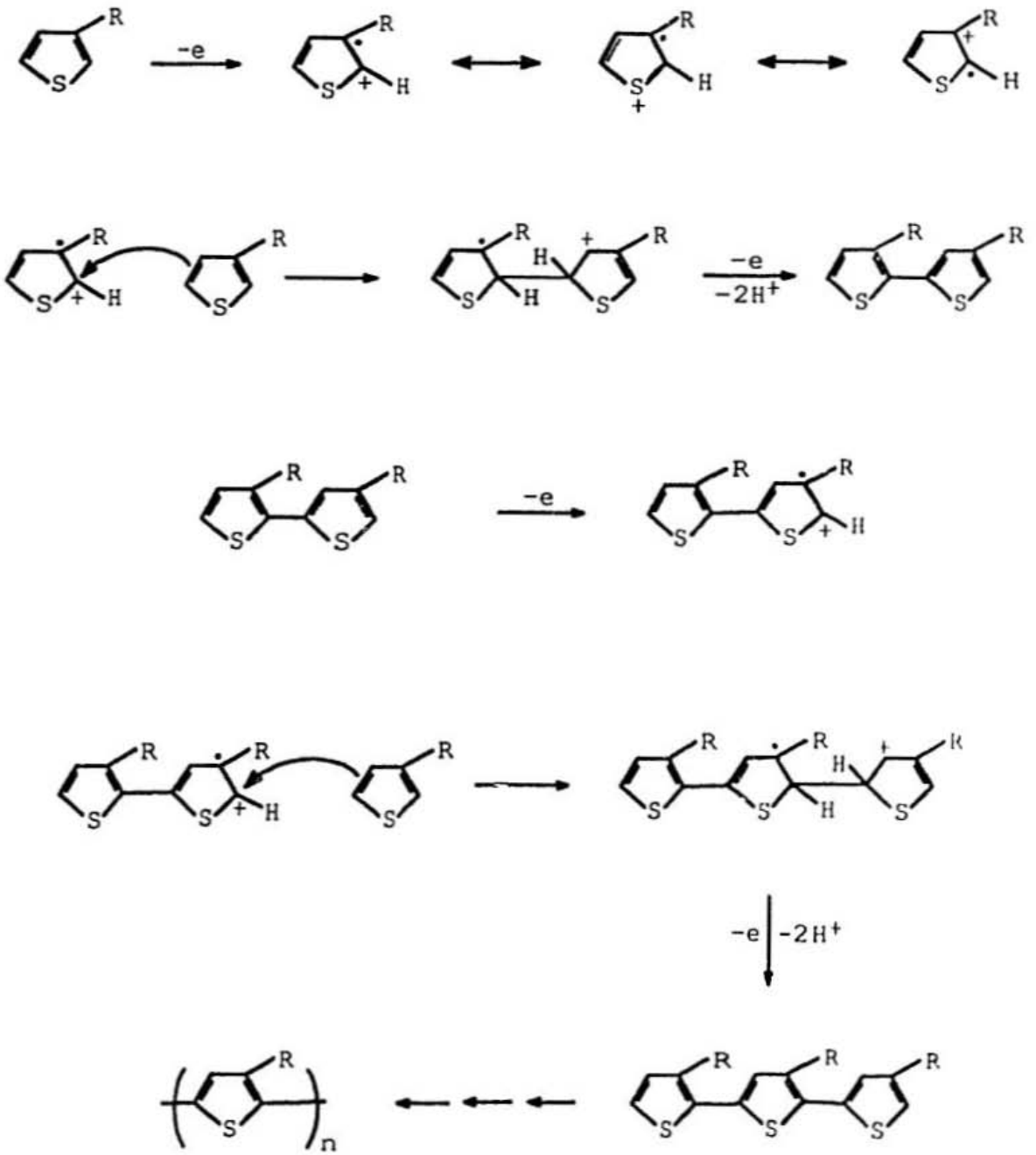

again the oxidation of the monomer to give a radical cation. In contrast to the radical-radical coupling mechanism presented in Scheme 1.1, the dimerization in this mechanism was supposed to take place through the electrophilic attack of the radical cation on a monomer, accompanied by further oxidation and deprotonation to generate the dimer. Polymer chain propagation involves the oxidation of monomeric or oligomeric species and further incorporation of monomer into the polymer chain, until the oligomers or polymers are large enough to be insoluble and deposit onto the electrode surface.

Wei et al.[45] obtained strong support for this mechanism by introducing a catalytic amount of dimeric or trimeric species into the synthesis solutions for the electropolymerization of thiophenes. As a result, not only were the oxidation potentials required for electropolymerization of thiophene and 3-alkylthiophenes dramatically decreased, but also the rate of polymerization was significantly enhanced. The radical-monomer coupling mechanism was used to rationalize these experimental observations, where the first step was presumed to be the oxidation of the additive at the lower potential, followed by coupling with the neutral monomer.

If coupling occurs on the electrode, as proposed by Marcos,[17] one-dimensional film growth should result from such a mechanism, where the number of active sites is proportional to the number of dimeric nuclei and will not be increased by the addition of a monomer to the end of a growing polymer chain. It is therefore difficult to explain the observed 3-dimensional growth of the polymer film, the increase in current with time in chronoamperometric transients, as well as the expansion of the electroactive surface area for electron transfer.[19] Furthermore, dendritic growth along the potential field toward the counter electrode would be expected for this mechanism, which was contrary to experimental results.[19]

1.3 Nucleation and Growth

Although the mechanisms discussed above are still topics of debate, it is now firmly established that the electropolymerization proceeds via some kind of nucleation and phase-growth mechanism, akin to the electrodeposition of metals.[19,22,37,40,54-56]

Both cyclic voltammetry and potential step techniques have been widely applied to investigate the mechanism of polymer electrodeposition. The electrochemical observations have been further supported by electron microscopy and various type of spectroscopy.[17,43,57,58]

1.3.1 Nucleation and Three-Dimensional Growth in the Early Stages

Hillman and co-workers[40] suggested that a monolayer of polymer is initially formed on which instantaneous nucleation and 3-dimensional growth then occurs. The large number of overlapping nuclei formed during the early stages of deposition leads to subsequent one-dimensional growth perpendicular to the electrode surface with a linear increase in thickness with time.[40,43] Other studies of the early stages of the deposition of polymer films also reported that the instantaneous creation of a high density of nucleation sites contributed to subsequent polymer generation and affected the polymer structure and morphology.[5]

Cyclic Voltammetric Evidence

In cyclic voltammetry studies, a ''nucleation loop'' is commonly observed,

where the current on the reverse scan is higher than on the corresponding forward scan, a characteristic phenomenon for a conducting phase formed by a nucleation and growth mechanism.[19,22,34,55]

Chronoamperometric Evidence

The electrodeposition of polymers by potential step techniques presents a well defined chronoamperometric response with a characteristic rising current-time (*I-t*) transient in the initial stages, followed by a steady state current. In the literature, the nucleation and growth processes have been investigated by analyzing the rising part in terms of i vs. t^n.[54] Most studies showed that the current i is proportional to t^2, indicating either an instantaneous nucleation with three-dimensional growth or successive nucleation with two-dimensional growth. Further investigation and calculations demonstrated that polymer growth occurs via instantaneous nucleation and three-dimensional growth.[19,22,40,55] Values of n of 1.5[54] and 3 or higher[41] have also been reported. Such values can arise from the three dimensional growth of nucleation sites, depending on the kinetics of nucleation, the rate-determining step, the diffusion of monomer to the electrode surface and electron transfer in the resulting polymer.[55] Three-dimensional growth was also considered to be confirmed by the trend to a steady current as the polymerization

proceeds.[35]

Morphological Evidence

Three-dimensional polymer growth was further supported by morphological investigations. The appearance of polypyrrole coated electrode surfaces in electron micrographs[35] and poly(3-methylthiophene) coated electrode surfaces in optical micrographs[46] shows the overlap of three-dimensional hemispherical nuclei of submicrometer diameter on the surface of resulting polymer films.

1.3.2 Polymer Growth

The dimers and oligomers formed via radical-radical coupling or radical-monomer coupling may precipitate as nucleation sites on the electrode surface, remain soluble in the vicinity of the electrode, or diffuse away from the electrode to the bulk solution. Therefore, polymer film formation can result from either the successive precipitation of oligomeric intermediates of lower solubility from the solution near the electrode, or from addition of monomers and oligomers to the ends of polymer chains adhering to the electrode surface.

The observation of monomer adsorption prior to the polymerization means that initiation of polymerization can take place on the electrode surface.[37] Baker and Reynolds have suggested that, when polymer formation occurs via three dimensional growth on a highly nucleated substrate, the primary reaction is the coupling of radical cations in solution with radical cations at chain ends in the polymer matrix.[18,57] Further insight into the polymer deposition was provided by Otero et al.,[32] who used rotating disc electrodes to investigate the electropolymerization of thiophene. A model of interfacial reactions involving oligomeric or polymeric species already grafted onto the electrode surface was proposed.

On the other hand, soluble oligomers have been reported to contribute to polymer deposition,[60,61] and their solubility affects the early stages of film formation.[38] Moreover, the presence of oligomeric intermediates in solution has been detected by UV-vis spectroscopy,[43,62] rotating ring-disc experiments[34] and the use of microelectrodes.[33] In these experiments, relatively stable monomeric or oligomeric species were observed diffusing away from the electrode surface before precipitation occurred. UV-vis studies revealed reactions forming longer soluble oligomeric products in the solution.[43,62] In addition, Garnier and co-workers[21]

reported that poly(3-methylthiophene) was formed through the generation of oligomeric species in the vicinity of the electrode, a preliminary step before their grafting onto the electrode surface. These studies confirm that polymer deposition can occur via precipitation of soluble oligomeric species from the solution. Thus although the role of oligomers in nucleation and deposition is still not fully understood, the expansion of nuclei can arise not only from the addition of monomers to polymer chain ends, but also from the precipitation of oligomeric intermediates formed in solution.

1.4 Objectives of This Work

The purpose of this study was to gain further insight into the mechanisms of polymer chain propagation and deposition. Poly(3-methylthiophene) has been electrochemically deposited on stationary and rotating electrodes by the potentiostatic technique, in an effort to confirm the formation of soluble oligomeric intermediates and to investigate the mechanism of electrodeposition under various conditions. We also applied cyclic voltammetry, impedance spectroscopy and scanning electron microscopy to characterize the resulting polymer films to obtain

further evidence. Thinner and more compact polymer films were generated on the rotating electrode as expected.

Moreover, a catalytic amount of 2,2'-bithiophene was introduced to solutions of 3-bromothiophene, seeking to decrease the oxidation potential required for poly(3-bromothiophene) formation and thus to enhance the overall rate of polymerization. Both cyclic voltammetry and x-ray emission spectroscopy were employed to compare the polymer films prepared in the absence and presence of 2,2'-bithiophene catalyst. Mechanisms have been proposed to rationalize the experimental observations. The effects of monomer and catalyst concentrations on the polymerization rate have also been studied.

References

1. L. Yu, M. Chen, and L.R. Dalton, *Chem. Mater.*, 1990, **2**, 649.

2. M. Kaneko and D. Wohrle, *Adv. Polym. Sci.*, 1988, **84**, 141.

3. M.G. Kanatzidis, *Chem. Eng. News*, 1990,, 36.

4. R.J. Waltman and J. Bargon, *Can. J. Chem.*, 1986, **64**, 76.

5. D. Curran, J. Grimshaw, and S.D. Perera, *Chem. Soc. Rev.*, 1991, **20**, 391.

6. H. Naarmann and N. Theophilou, in *Electroresponsive Molecular and Polymeric Systems*, vol. 1, T.A. Skotheim, Ed. (Marcel Dekker, New York, 1988), pp. 1-39.

7. A. Techagumpuch, H.S. Nalwa, and S. Miyata, in *Electroresponsive Molecular and Polymeric Systems*, vol. 2, T.A. Skotheim, Ed. (Marcel Dekker, New York, 1991), pp. 257-294.

8. J. Heinze, in *Topics in Current Chemistry*, vol. 152. (Springer-Verlag, Berlin, 1990), pp. 1-47.

9. A. Dall'Olio, Y. Dascola, V. Varacca, and V. Bocchi, *C.R. Acad. Sci. Ser. C*, 1968, **267**, 433.

10. A.F. Diaz and K.K. Kanazawa, in *Extended Linear Chain Compounds*, vol. 3, J.S. Miller, Ed. (,, 1982), pp. 417-441.

11. G.B. Street, in *Handbook of Conducting Polymers*, vol. 1, T.A. Skotheim, Ed. (Marcel Dekker, New York, 1986), pp. 265-292.

12. J. Roncali, *Chem. Rev.*, 1992, **92**, 711.

13. G. Tourillon, in *Handbook of Conducting Polymers*, vol. 1, T.A. Skotheim, Ed. (Marcel Dekker, New York, 1986), pp. 293-350.

14. R.J. Waltman and J. Bargon. *Tetrahedron*. 1984, **40**, 3963.

15. A.F. Diaz, J.I. Castillo, J.A. Logan, and W.-Y. Lee, *J. Electroanal. Chem.*, 1981, **129**, 115.

16. R.J. Waltman, J. Bargon, and A.F. Diaz, *J. Phys. Chem.*, 1983, **87**, 1459.

17. E.M. Genies, G. Bidan, and A.F. Diaz, *J. Electroanal. Chem.*, 1983, **149**, 101.

18. C.K. Baker and J.R. Reynolds, *J. Electroanal. Chem.*, 1988, **251**, 307.

19. S. Asavapiriyanont, G.K. Chandler, G.A. Gunawardena, and D. Pletcher, *J. Electroanal. Chem.*, 1984, **177**, 229.

20. L. Laguren-Davidson, C.V. Pham, H. Zimmer, H.B. Mark Jr., and D.J. Ondrus, *J. Electrochem. Soc.*, 1988, **135**, 1406.

21. J. Roncali, F. Garnier, M. Lemaire, and R. Garreau, *Synth. Met.*, 1986, **15**, 323.

22. A.J. Downard and D. Pletcher, *J. Electroanal. Chem.*, 1986, **206**, 147.

23. J. Roncali, M. Lemaire, R. Garreau, and Garnier, *Synth. Met.*, 1987, **18**, 139.

24. P. Lang, F. Chao, M. Costa, E. Lheritier, and F. Garnier, *Ber. Bunsenges. Phys. Chem.*, 1988, **92**, 1528.

25. G.K. Chandler and D. Pletcher, *Spec. Period. Rep. Electrochem.*, 1985, **10**, 117.

26. A.F. Diaz, J.F. Rubinson, and H.B. Mark Jr., *Adv. Polym. Sci.*, 1988, **84**, 113.

27. J. Heinze, *Synth. Met.*, 1991, **41-43**, 2805.

28. F. Beck, P. Braun, and M. Oberst, *Ber. Bunsenges. Phys. Chem.*, 1987, **91**, 967.

29. F. Beck, P. Braun, and Schloten, *J. Electroanal. Chem.*, 1989, **267**, 141.

30. E.W. Tsai, S. Basak, J.P. Ruiz, J.R. Reynolds, and K. Rajeshwar, *J. Electrochem. Soc.*, 1989, **136**, 3683.

31. G. Tourillon and F. Garnier, *J. Phys. Chem.*, 1983, **87**, 2289.

32. T.F. Otero and J. Rodriguez, *J. Electroanal. Chem.*, 1991, **310**, 219.

33. R. John and G.G. Wallace, *J. Electroanal. Chem.*, 1991, **306**, 157.

34. K. Tanaka, T. Shichiri, S. Wang, and T. Yamabe, *Synth. Met.*, 1988, **24**, 203.

35. D.E. Raymond and D.J. Harrison, *J. Electroanal. Chem.*, 1990, **296**, 269.

36. F. Beck, M. Oberst, and R. Jansen, *Electrochimica Acta*, 1990, **35**, 1841.

37. M.L. Marcos, I. Rodriguez, and J. Gonzalez-Velasco, *Electrochimica Acta*, 1987, **32**, 1453.

38. B.R. Scharifker, E. Garciapastoriza, and W. Marino, *J. Electroanal. Chem.*, 1991, **300**, 85.

39. R. John and G.G. Wallace, *Polymer International*, 1992, **27**, 255.

40. A.R. Hillman and E.F. Mallen, *J. Electroanal. Chem.*, 1987, **220**, 351.

41. C.K. Baker and J.R. Reynolds, *ACS, Polym. Chem., Polymer Reprints*, 1987, **28**, 284.

42. Y.J. Qiu and J.R. Reynolds, *J. Pol. Sci., Part A, Pol. Chem.*, 1992, **30**, 1315.

43. A.R. Hillman and M.J. Swann, *Electrochimica Acta*, 1988, **33**, 1303.

44. C.P. Andrieux, P. Audebert, P. Hapiot, and J.-M. Saveant, *J. Am. Chem. Soc.*, 1990, **112**, 2439.

45. Y. Wei, C.-C. Chan, J. Tian, G.-W. Jang, and K.F. Hsueh, *Chem. Mater.*, 1991, **3**, 888.

46. J. Lukkari, R. Tuomala, S. Ristimaki, and J. Kankare, *Synth. Met.*, 1992, **47**, 217.

47. A.F. Diaz, J. Crowley, J. Bargon, G.P. Gardini, and J.B. Torrance, *J. Electroanal. Chem.*, 1981, **121**, 355.

48. D.D. Cunningham, L. Laguren-Davidson, H.B. Mark, C.V. Pham, and H. Zimmer, *J. Chem. Soc., Chem. Commun.*, 1987,, 1021.

49. A. Galal, E.T. Lewis, O.Y. Ataman, H. Zimmer, and H.B. Mark, *J. Pol. Sci., Part A, Pol. Chem.*, 1989, **27**, 1891.

50. J. Heinze, M. Storzbach, and J. Mortensen, *J. Electroanal. Chem.*, 1984, **165**, 61.

51. K. Tanaka, T. Shichiri, M. Toriumi, and T. Yamabe, *Synth. Met.*, 1989, **30**, 271.

52. E.M. Genies and A. Diaz, *J. Electroanal. Chem.*, 1979, **98**, 305.

53. J. Ochmanska and P.G. Pickup, *J. Electroanal. Chem.*, 1989, **271**, 83.

54. F.B. Li and W.J. Albery, *Electrochimica Acta*, 1992, **37**, 393.

55. R.E. Noftle and D. Pletcher, *J. Electroanal. Chem.*, 1987, **227**, 229.

56. A.J. Downard and D. Pletcher, *J. Electroanal. Chem.*, 1986, **206**, 139.

57. P.A. Christensen, A. Hamnett, and A.R. Hillman, *J. Electroanal. Chem.*, 1988, **242**, 47.

58. A.R. Hillman, E.F. Mallen, and A. Hamnett, *J. Electroanal. Chem.*, 1988, **244**, 353.

59. I. Rodriguez, M.L. Marcos, and J. Gonzalez-Velasco, *Electrochimica Acta*, 1987, **32**, 1181.

60. P. Lang, F. Chao, M. Costa, and F. Garnier, *Polymer*, 1987, **28**, 668.

61. A. Hamnett and A.R. Hillman, *J. Electrochem. Soc.*, 1988, **135**, 2517.

62. A.R. Hilman and E. Mallen, *J. Electroanal. Chem.*, 1988, **243**, 403.

63. A. Hamnett, S.J. Higgins, P.R. Fisk, and W.J. Albery, *J. Electroanal. Chem.*, 1989, **270**, 479.

64. S. Servagent and E. Vieil, *J. Electroanal. Chem.*, 1990, **280**, 227.

Chapter 2

Experimental

2.1 Chemicals and Monomer Solutions

3-methylthiophene (Aldrich) and 3-bromothiophene (Aldrich) were distilled under reduced pressure before use. 2,2'-bithiophene (Aldrich) was recrystallized from ethanol. Acetonitrile (Fisher HPLC grade or Caledon Reagent Grade) and acetone (ACS, Fisher) were used without any further purification. The water content of each type of acetonitrile was estimated by IR and compared with the data provided by the manufacturer. Tetraethylammonium perchlorate (Et_4NClO_4, purum, Fluka) was dried in a vacuum at 100° C for over 48 h. Tetrabutylammonium hexaflurophosphate (Bu_4NPF_6, puriss.p.a., Fluka) and lithium perchlorate ($LiClO_4$, Aldrich) were used as received.

3-methylthiophene monomer solutions in acetonitrile (Fisher) were prepared every two or three days and stored at room temperature. 3-bromothiophene solutions in acetonitrile (Fisher or Caledon) were prepared every day and

sometimes immediately before the experiment. A fresh solution was used for each experiment to prevent interference from oligomers produced in a previous experiment.

2.2 Electrochemistry

2.2.1 Electrodes, Cells and Instrumentation

A platinum rotating disc electrode (RDE) with an area of 0.0071 cm^2 sealed in PTFE was employed as the working electrode in all experiments. A Ag/AgCl/0.1 M Cl(aq.) reference electrode with a saturated Et_4NClO_4(aq.) salt bridge was used in the preparation of poly(3-methylthiophene) and in the characterization of the resulting polymer films by cyclic voltammetry, while a saturated sodium chloride calomel electrode (SSCE) was used in all other experiments. A Pt wire was used as the counter electrode in all studies.

All electrochemical experiments were carried out in three-compartment glass cells in air. The reference-electrode compartment was connected to the main

compartment through a Luggin capillary. Results of preliminary studies carried out under argon were not significantly different from those in air, indicating no interference from oxygen in the potential range employed. A Model CS-1090 computer-controlled electroanalytical system (Cypress Systems, Inc.) combined with an analytical rotator (Pine Instrumental Company) was used for the work on poly(3-methylthiophene), while a Pine Instruments RDE4 potentiostat/galvanostat connected with a HB-111 Hokuto Denko function generator, a BBC SE 780 X-Y recorder and a digital to analogue converter of a Tatung TCS-7000 computer was used for the work on poly(3-bromothiophene).

The integration of the cathodic parts of cyclic voltammograms recorded during the polymerization of 3-bromothiophene was performed using a Tatung TCS-7000 computer, a Data Translation DT2801 ADC/DAC card and a self-written program called QT. QT collects ca. 8 data points per second to sample the current-potential curve; it starts integration during each cycle when the current becomes negative and stops at the end of the cathodic scan.

Impedance spectroscopy was performed using a Model 1250 Solartron Frequency Response Analyzer connected with a Model 1286 Solartron

Electrochemical Interface. An a.c. potential stimulation of 5 mV r.m.s. was used in the impedance measurements. Data were sampled from high to low frequency over the range of 20 kHz-0.1 Hz, and analyzed using an Laser 80286 microcomputer and ZPLOT software (Scribner associates Inc.)

2.2.2 Electrode Pretreatment

The electrode was polished with Linde A 0.3 μm alumina (Micro Metallurgical Ltd.) on Rayfinal microcloth (Micro Metallurgical Ltd.), and then rinsed with distilled water and acetone. The Pt electrode was further treated by cycling in a monomer-free solution for several scans, from -0.5 to 2.0 V at 50 mV/s and stopped at 0 V, in an effort to ensure no polymer remained on the electrode surface. The pretreated electrode was rinsed again with acetone in an ultrasonic bath for several seconds.

2.3 Electrochemical Characterization of Polymer Films

2.3.1 Cyclic Voltammetry

Polymer films were studied in a monomer-free $LiClO_4$/acetonitrile solution, or Bu_4NPF_6/acetonitrile solution. Samples were thoroughly rinsed with acetone after synthesis, and allowed to dry in air prior to cyclic voltammetry. The poly(3-methylthiophene) films were cycled in a potential range of -0.4 to 1.0 V at a scan rate of 100 mV/s, and only the second scan was recorded for each film. The cycling charges were obtained by integrating the anodic or the cathodic part of the cyclic voltammogram.

2.3.2 Impedance Spectroscopy

The poly(3-methylthiophene) coated electrodes were pretreated by cyclic voltammetry before starting impedance measurements at +1.0 V in the same electrolyte solution . The uncompensated solution resistance was obtained from the intercept of an imaginary impedance (Z'') vs. real impedance (Z') plot for a bare Pt electrode at the real impedance axis.

2.4 Scanning Electron Microscopy and X-ray Emission Spectroscopy

2.4.1 Morphological Studies

The morphology of poly(3-methylthiophene) coated electrode surfaces was examined using a Hitachi S-570 scanning electron microscope. The electrodes were thoroughly rinsed with acetone after preparation, and dried in air before examination. The accelerating voltage was set at 20 kV.

2.4.2 X-ray Emission Analysis

X-ray emission spectra were obtained using a Hitachi S-570 scanning electron microscope equipped with a Tracor Northern 5500 Energy Dispersive X-ray analyzer and a Microtrace 70152 silicon detector. An accelerating voltage of 20 kV was used. The polymer coated electrodes were rinsed with acetone and dried in air after synthesis. All polymer films were peeled off the electrode surface with small pieces of Scotch tape, in order to avoid any interference from the Pt substrate. A piece of tape was examined in a preliminary experiment and showed an absence of peaks and a very low background.

Tracor Northern's Standardless Quantitative analysis (SQ) software package

was applied to calculate relative elemental concentrations of the polymer films. This program performs peak area measurements, a background correction, corrections for matrix effects and calculations of relative peak intensities and relative elemental concentrations. In particular, a so-called ZAF correction[1,2] is applied, where Z stands for the influence of the atomic number, A for the absorption of x-rays by the matrix and F for the fluorescence x-ray emitted by the matrix.

References

1. M.T. Postek Jr., K.S. Howard, A.H. Johnson, and K.L. McMichael, *Scanning Electron Microscopy: A Student's Handbook* (Ladd Research Industries, Inc., 1980).

2. *Energy-Dispersive X-ray Microanalysis: An Introduction* (Kevex Corporation, Foster City, California, 1983).

Chapter 3

A Rotating Disc Electrode Study of the Electrodeposition of Poly(3-Methylthiophene)

3.1 Introduction

As discussed in Chapter 1, the mechanism of electropolymerization and deposition of heterocyclic monomers has been the subject of intense research. Although it has been firmly established that the polymer formation takes place via a nucleation and growth mechanism (Section 1.3.1), the exact processes involved in polymer chain propagation and polymer deposition on the electrode surface are still topics of debate. It has been shown that polymer deposition can result from precipitation of oligomeric intermediates from the synthesis solution, and/or from sequential coupling of monomers or monomeric radical cations to polymer chains grafted to the electrode (Section 1.3.2).

Rotating disc electrodes (RDE) and rotating ring-disc electrodes (RRDE)

have been previously used in a few studies on conducting polymers, for the purpose of detecting soluble oligomeric species produced during polymerization[44] or determining the nature of the kinetics of polymerization[45]. In this work, a rotating Pt disc electrode was used to investigate the potentiostatic electropolymerization of 3-methylthiophene, in an effort to elucidate the mechanism of polymer deposition, especially at relative long polymerization times (*i.e.*, 3 min. in most experiments of this study), where thick polymer films were produced.

3.2 Results

3.2.1 Electropolymerization of 3-Methylthiophene under Various Conditions

3.2.1.1 Polymer Generation on Stationary and Rotating Electrodes

Figure 3.1 illustrates chronoamperometric responses (*I-t* curves) to a potential step from 0 V to 1.25 V. The experiments were carried out in a solution of 0.1 M $LiClO_4$/acetonitrile containing 0.1 M 3-methylthiophene, using a stationary Pt electrode (Fig. 3.1a) as well as a rotating electrode at different rotation

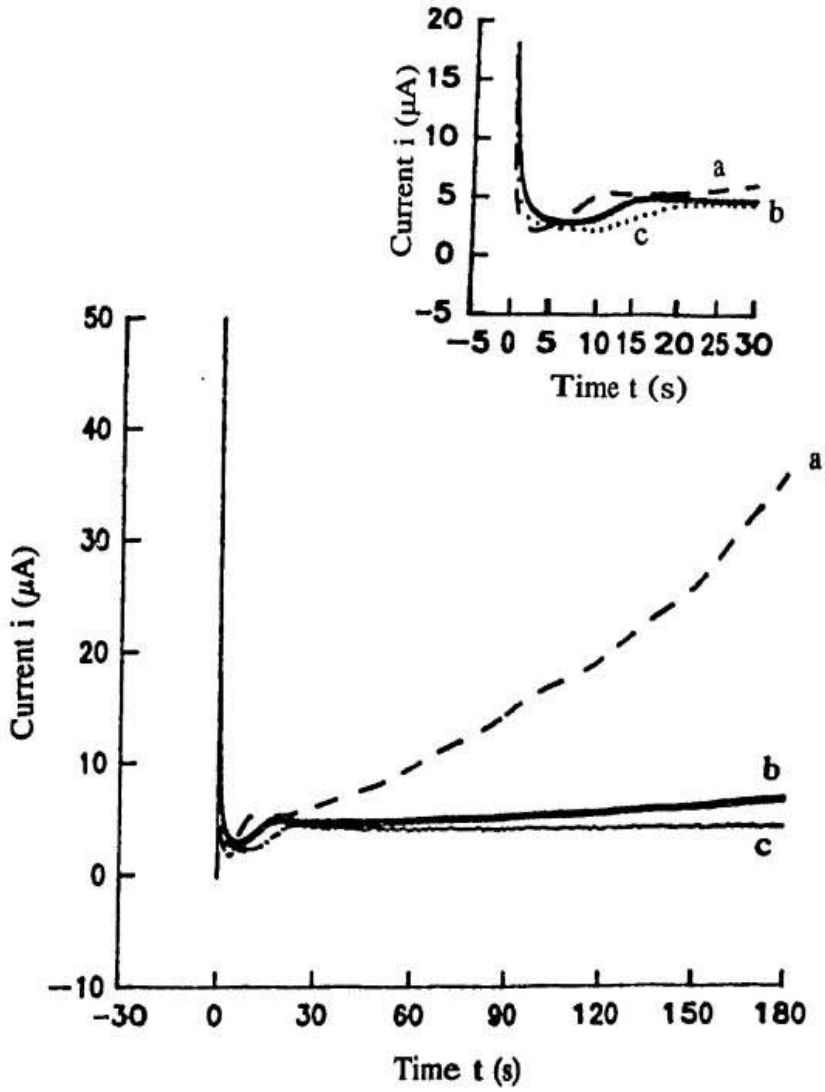

Figure 3.1 Current-time plots for electropolymerization of 0.1 M 3-methylthiophene in 0.1 M $LiClO_4/CH_3CN$ on a Pt RDE at rotation rates of (a) 0 rpm; (b) 400 rpm and (c) 1600 rpm. The potential was stepped from 0 to 1.25 V.

rates (Fig. 3.1b and 3.1c). In general, each individual *I-t* transient has the characteristic form observed for electropolymerization under potentiostatic conditions.[6,7] An initial current spike due to a charging process appears immediately after the application of the potential step. The current then falls sharply, followed by a longer rising transient. The current decay does not simply result from the charging of the double layer, but also from other processes such as monomer adsorption at the electrode/solution interface,[8] a nucleation/growth process and soluble oligomer formation.[7,8]

The rising transient following the initial current spike has been attributed to the nucleation and subsequent growth of the polymer film.[7] To diagnose the nature of polymer formation during this initial rising portion of the *I-t* curve , an approach from the literature[4,7] has been adopted, where the minimum is used as the time and current zero for the rising transient. Data corrected in this way were plotted as log *i* vs. log *t*. Figure 3.2 presents an example of determination of the relationship between the current and the polymerization time for the rising transient shown in Figure 3.1a. Slopes of these linear lines were ca. 2 for the three sets of data in Figure 3.1, indicating either two-dimensional progressive nucleation and growth, or three-dimensional instantaneous nucleation and growth.[7,9,10]

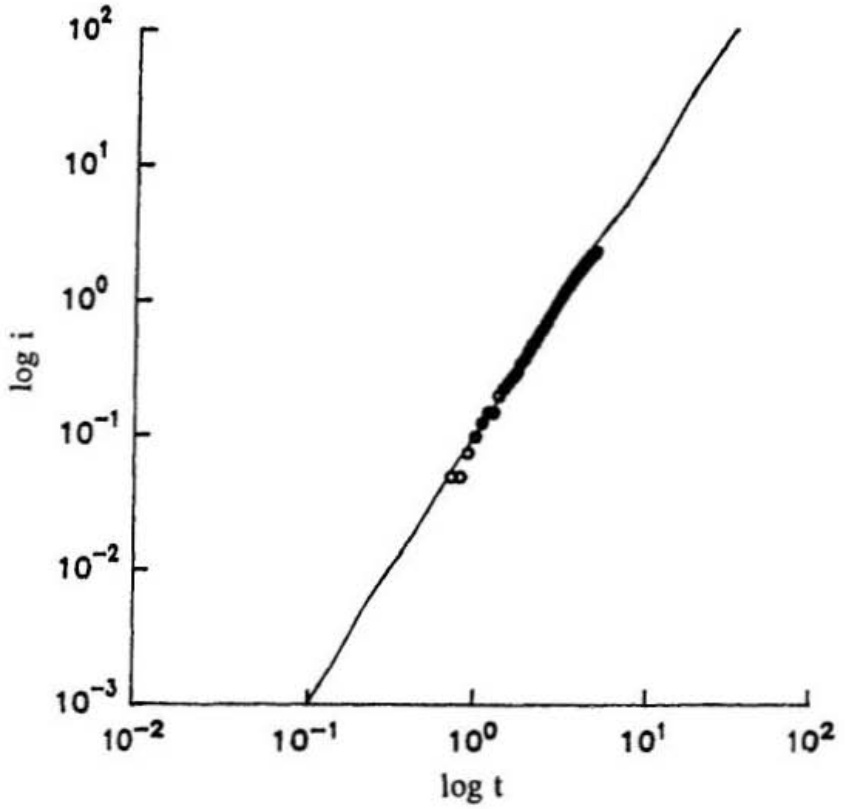

Figure 3.2 Determination of the relationship between the current and the polymerization time for the initial rising transient shown in Figure 3.1a.

For the stationary electrode, a small plateau was observed after the rising portion (> ca. 10 s as shown in Fig. 3.1a) as described in previous studies,[7,10] but then the current increased significantly at longer times. This behaviour changed drastically when the electrode was rotated. Figure 3.1b shows a slower current increase with polymerization time at a rotation rate of 400 rpm. At higher rotation rate (*i.e.*, 1600 rpm in Fig. 3.1c), the current levels off towards an almost steady state current through the rest of polymerization. By comparing the early stages of the three curves in Figure 3.1, different times were observed for the initial spike to decay to a minimum, and for the rising transient to peak. These initial stages take notably longer at increasing rotation rates, which indicates that the creation and expansion of the polymer nuclei occur more slowly at high rotation rates.

Further insight into the influence of rotation on the preparation of poly(3-methylthiophene) was obtained by initiating rotation at a certain time of polymerization on a stationary electrode (Fig. 3.3) and by stopping rotation after a certain polymerization time (Fig. 3.4).

In Figure 3.3, curves a to d are similar in the early stages because the electrode was kept stationary, but different from curve e where the electrode was

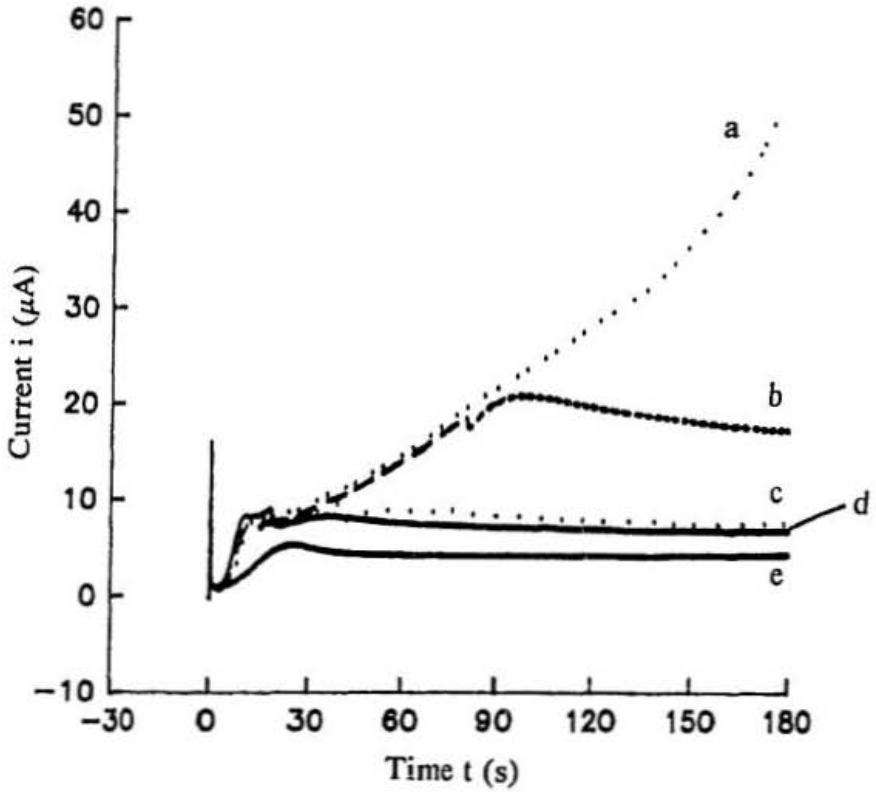

Figure 3.3 Current-time plots for the electropolymerization of 0.1 M 3-methylthiophene in 0.1 M $LiClO_4/CH_3CN$ started on a stationary Pt RDE, and then rotated at (a) NA (*i.e.*, only stationary electrode was used); (b) 80 s; (c) 40 s; (d) 20 s and (e) 0 s at a rotation rate of 1600 rpm.

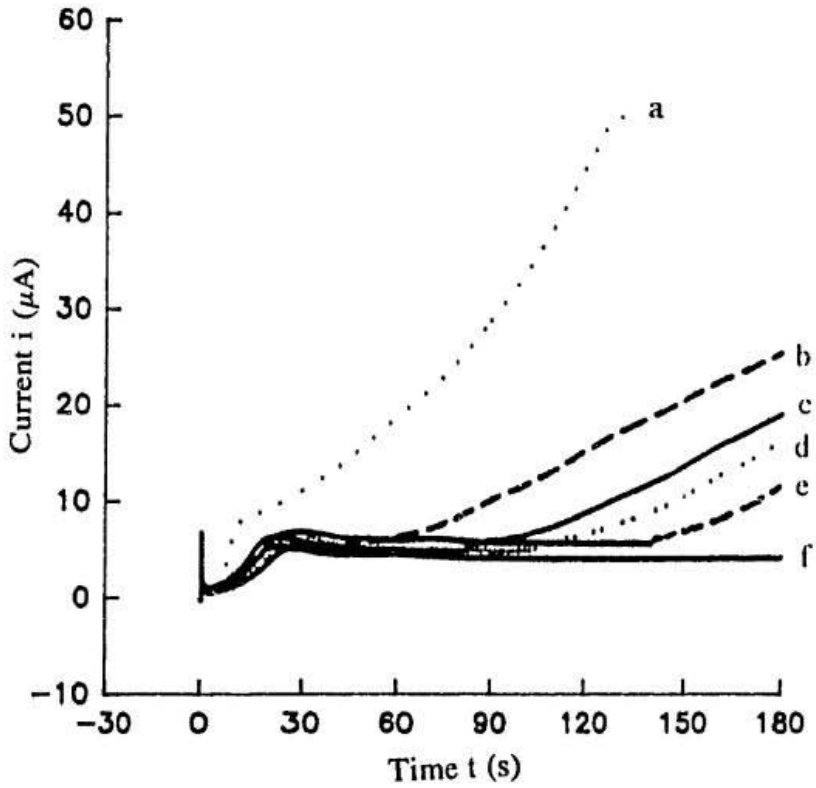

Figure 3.4 Current-time plots for the electropolymerization of 0.1 M 3-methylthiophene in 0.1 M $LiClO_4/CH_3CN$ started on a Pt RDE at a rotation rate of 1600 rpm, and then stopped rotation at (a) 0 s; (b) 40 s; (c) 80 s; (d) 100 s; (e) 140 s and (f) NA (*i.e.*, only rotating electrode was used).

rotated. When the electrode started to rotate in experiments b, c and d, the current decreased gradually towards a steady state after a small falling and then rising transient. It is clear that earlier rotation leads to a lower current as polymerization proceeds.

The other set of experiments gave the reverse behaviour, as shown in Figure 3.4. In five out of the six experiments, the polymerization was started at a rotating electrode, the transients are therefore similar in the early stages, and the current levels off after the initial rising transient. But a dramatic increase in current was observed when the electrode rotation was stopped. A small step in current appears at the moment of change with a gradual increase in current followed by a much faster rising transient.

3.2.1.2 Effect of Applied Potential on the Electropolymerization

Prior studies indicated that an increase in the applied potential in the potential step experiment increases the polymer growth rate.[6,11,12] *I-t* responses for the electropolymerization of 3-methylthiophene at different potentials were recorded at both stationary and rotating (900 rpm) electrodes, as shown in Figures 3.5 and

3.6, respectively. In agreement with the earlier works, an overall increase in current was observed as the applied oxidation potential was increased. The initial current spike and decay is followed by a slow rise at lower potentials and a relatively rapid rise at higher potentials. The time required for the initial current to reach the minimum as well as for the rising transient to peak is shortened as the applied potential is increased. Following a small plateau, the current increases much more rapidly at higher potentials.

Comparing Figure 3.6 with Figure 3.5, it is clear that higher potentials are required to generate polymer on a rotating electrode. Even so, at high potentials (Fig. 3.6a), a continuously rising current similar to that obtained for a stationary electrode can be observed during rotation.

3.2.1.3 Polymer Generation in the Et_4NClO_4/Acetonitrile Medium

Similar experimental results have been obtained for the electropolymerization of 3-methylthiophene in 0.1 M Et_4NClO_4/acetonitrile solution, using stationary and rotating electrodes. Figure 3.7 shows typical chronoamperometric responses for the electropolymerization of 0.1 M 3-methylthiophene under various conditions.

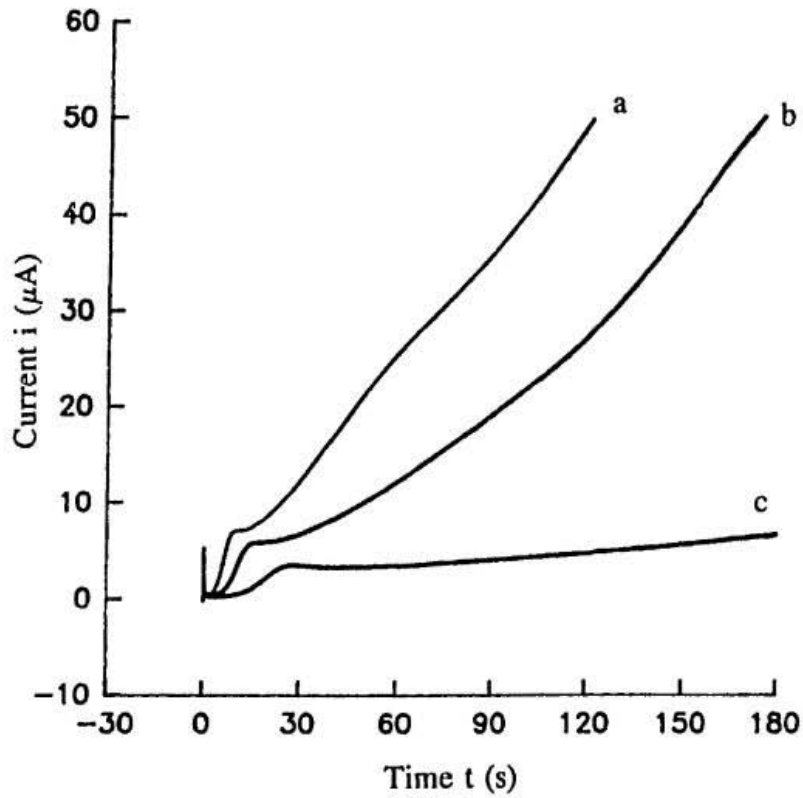

Figure 3.5 Current-time plots for the electropolymerization of 0.1 M 3-methylthiophene in 0.1 M $LiClO_4/CH_3CN$ on a Pt stationary electrode under the potential steps from 0 V to (a) 1.25 V; (b) 1.24 V and (c) 1.22 V.

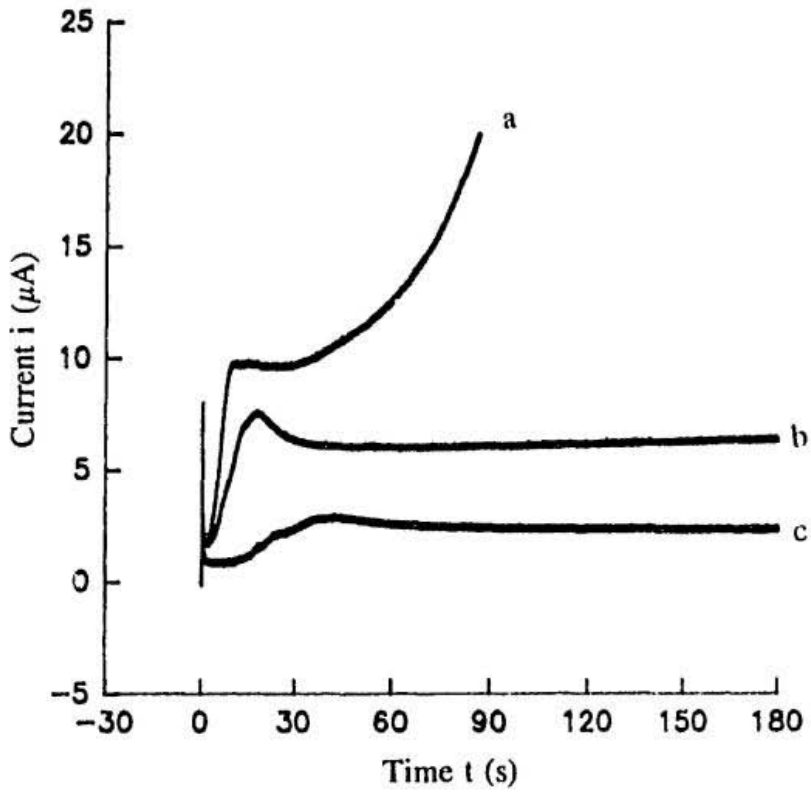

Figure 3.6 Current-time plots for the electropolymerization of 0.1 M 3-methylthiophene in 0.1 M $LiClO_4/CH_3CN$ on a Pt RDE at a rotation rate of 900 rpm under the potential steps from 0 V to (a) 1.27 V; (b) 1.25 V and (c) 1.23 V.

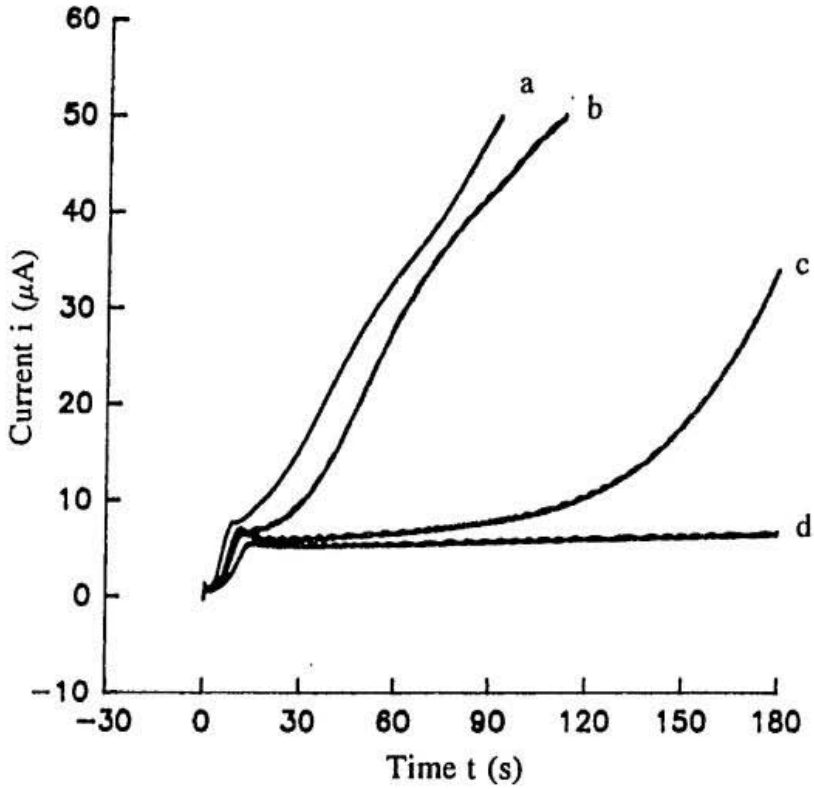

Figure 3.7 Current-time plots for the electropolymerization of 0.1 M 3-methylthiophene in 0.1 M Et_4NClO_4/CH_3CN on a Pt RDE at rotation rates of (a) 0 rpm; (b) 400 rpm; (c) 900 rpm and (d) 1600 rpm. The potential was stepped from 0 to 1.29 V.

Analogous to Figure 3.1, longer initial stages and lower currents were obtained with increasing rotation rate. However, the differences between curves recorded for the stationary electrode (Fig. 3.7a) and for the electrode rotating at 400 rpm (Fig. 3.7b) are much smaller than those observed when the electrolyte was $LiClO_4$.

3.2.2 Electrochemical Characterization of Resulting Polymers

3.2.2.1 Cyclic Voltammetric Studies

Figure 3.8 shows cyclic voltammograms for the poly(3-methylthiophene) films prepared in the experiments of Figure 3.1, in a 0.1 M $LiClO_4$/acetonitrile solution. In all cases, typical redox waves for poly(3-methylthiophene) were observed, in which both anodic and cathodic peaks are broad. Since peak currents are proportional to the amount of polymer on the electrode, it is clear that more polymer was formed on the stationary electrode, and that the amount of polymer deposited on the electrode surface decreases with increasing rotation rate during preparation. The decrease in polymer generation in the stirred solution is consistent with the current-time transients presented in Figure 3.1.

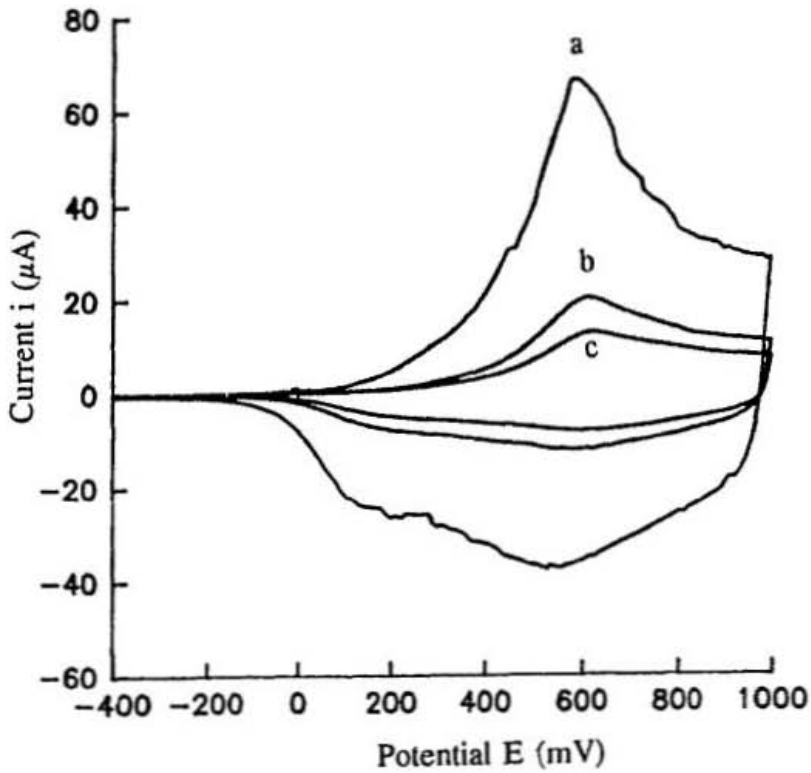

Figure 3.8 Cyclic voltammograms for the poly(3-methylthiophene) coated electrodes prepared in Figure 3.1. The scan rate was 100 mV/s. (a) refers to the polymer prepared on a stationary electrode; (b) refers to the polymer prepared on a rotating electrode at 400 rpm and (c) refers to the polymer prepared on a rotating electrode at 1600 rpm.

Cyclic voltammograms of polymers prepared under the conditions illustrated in Figures 3.3 and 3.4 are shown in Figures 3.9 and 3.10, respectively. Characteristic redox waves were observed in each individual cyclic voltammogram, indicating that a film of poly(3-methylthiophene) had been produced. In both experiments, peak currents decrease as the proportion of time with the electrode rotating during the polymerization is increased, and thus the amount of polymer on the electrode decreases.

The deposition of a poly(3-methylthiophene) film in its oxidized state usually consumes 2.25-2.4 F/mol, while doping of the polymer involves ca. 0.3 F/mol (Section 1.1). Therefore, the charge required for film doping is normally ca. 13% of the polymerization charge. A process less than 100% efficient would produce less polymer for a certain polymerization charge and so the cycling to polymerization charge would be less than 0.13. Consequently, the coulombic efficiency of a certain electropolymerization process can be obtained from the ratio of the doping charge to the total polymerization charge divided by 0.13.

The cycling charge passed during polymer oxidation or reduction in a monomer-free solution represents the charge required for film doping, and is

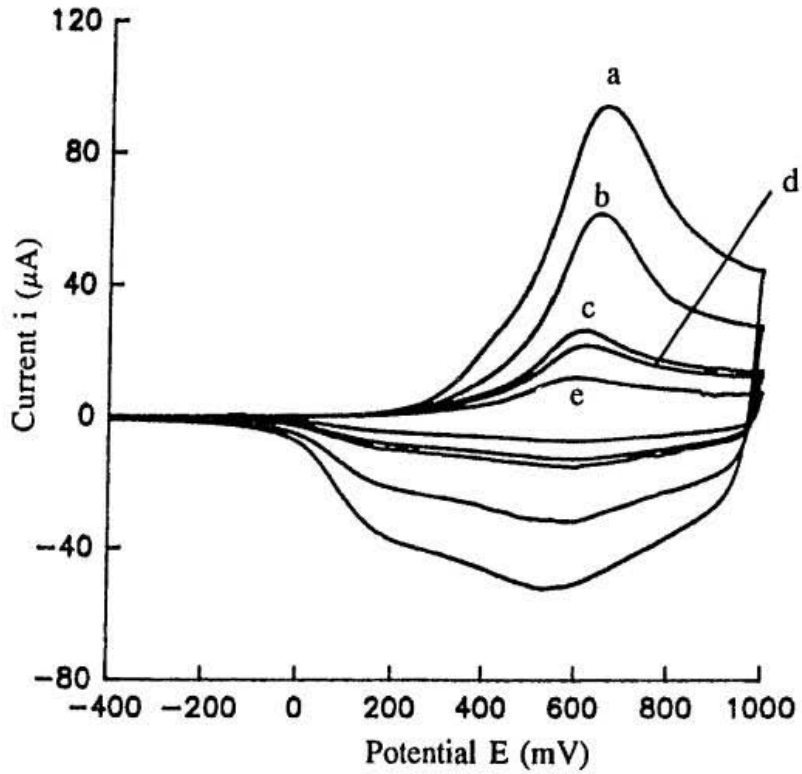

Figure 3.9 Cyclic voltammograms for the poly(3-methylthiophene) coated electrodes prepared in Figure 3.3. The scan rate was 100 mV/s. (a) refers to the polymer prepared on a stationary electrode; (b) to (d) refer to the polymers prepared first on a stationary electrode and then started rotation at 1600 rpm at polymerization time of (b) 80 s; (c) 40 s and (d) 20 s; (e) refers to the polymer prepared on a rotating electrode at 1600 rpm.

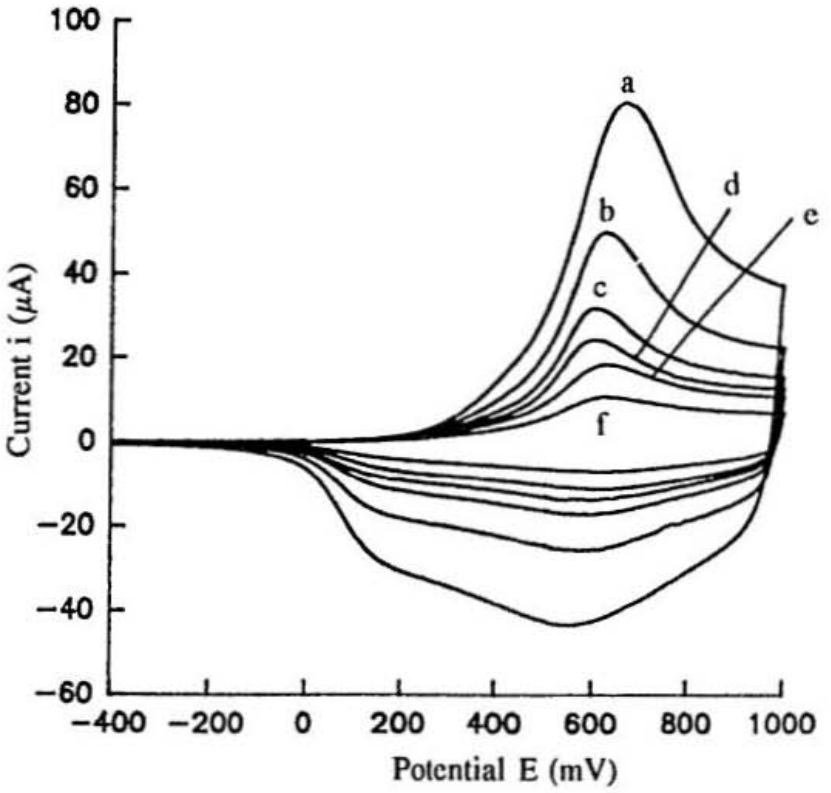

Figure 3.10 Cyclic voltammograms for the poly(3-methylthiophene) coated electrodes prepared in Figure 3.4. The scan rate was 100 mV/s. (a) refers to the polymer prepared on a stationary electrode; (b) to (e) refer to the polymers prepared first on a rotating electrode at 1600 rpm and then stopped rotation at polymerization time of (b) 40 s; (c) 80 s; (d) 100 s and (e) 140 s. (f) refers to the polymer prepared on a rotating electrode at 1600 rpm.

proportional to the amount of polymer deposited on the electrode.[13] The total charge consumed during polymer formation can be obtained by integration of a current-time transient, and the cycling charge stored in the polymer can be measured by integrating either the oxidation or the reduction part of a corresponding cyclic voltammogram.

Tables 3.1, 3.2, 3.3 and 3.4 list the polymerization charges, cycling charges and coulombic efficiencies for the polymer films prepared in the experiments illustrated by Figures 3.1, 3.3, 3.4 and 3.7, respectively. In Tables 3.1 and 3.4, it can be seen that the polymerization charge decreases and less polymer is produced (*i.e.*, less cycling charge) with increasing rotation rate of the RDE. Moreover, a decrease in coulombic efficiency was observed as the rotation rate was increased. It should also be pointed out that both the polymerization charge and the cycling charge dropped drastically when the electrode was rotated (Table 3.1). In comparison, the changes observed with varying rotation rate were relatively small. In Table 3.4, there is little difference in the polymerization charges and cycling charges between the polymerization on the stationary electrode and on the rotating electrode at 400 rpm. Much less charge was consumed by polymerization and stored in the polymer matrix at higher rotation rates.

Table 3.1 Polymerization charges, cycling charges and coulombic efficiencies of polymerization for the polymer films prepared in the experiments of Figure 3.1

Curve No.	Rotation Rate ω (rpm)	Polymerization Charge $Q_{pol.}$ (mC)	Cycling Charge		Coulombic Efficiency	
			$Q_{ox.}$ (μC)	$Q_{red.}$ (μC)	from $Q_{ox.}/Q_{pol.}$ (%)	from $Q_{red.}/Q_{pol.}$ (%)
a	0	2.804	275.2	269.9	75.5	74.0
b	400	0.953	87.4	85.3	70.5	68.9
c	1600	0.726	58.0	55.9	61.5	59.2

Total polymerization time = 180 s
Electrolyte : $LiClO_4$

Table 3.2 Polymerization charges, cycling charges and coulombic efficiencies of polymerization for the polymer films prepared in the experiments of Figure 3.3

Curve No.	Rotation time t (s)	Polymerization Charge $Q_{pol.}$ (mC)	Cycling Charge		Coulombic Efficiency	
			$Q_{ox.}$ (μC)	$Q_{red.}$ (μC)	from $Q_{ox.}/Q_{pol.}$ (%)	from $Q_{red.}/Q_{pol.}$ (%)
a	0	4.102	376.9	373.5	70.7	70.0
b	100	2.730	231.0	228.2	65.1	64.3
c	140	1.398	110.8	108.6	61.0	59.8
d	160	1.274	95.7	93.2	57.8	56.3
e	180	0.741	55.1	52.3	57.2	54.3

Total polymerization time = 180 s
Electrolyte : $LiClO_4$
Rotation rate : 1600 rpm

Table 3.3 Polymerization charges, cycling charges and coulombic efficiencies of polymerization for the polymer films prepared in the experiments of Figure 3.4

Curve No.	Rotation time t (s)	Polymerization Charge $Q_{pol.}$ (mC)	Cycling Charge		Coulombic Efficiency	
			$Q_{ox.}$ (μC)	$Q_{red.}$ (μC)	from $Q_{ox.}/Q_{pol.}$ (%)	from $Q_{red.}/Q_{pol.}$ (%)
b	40	2.114	189.7	186.2	69.0	67.8
c	80	1.478	126.3	122.6	65.7	63.8
d	100	1.225	100.7	97.8	63.2	61.4
e	140	1.107	81.3	78.5	56.5	54.5
f	180	0.724	51.0	48.4	54.2	51 4

Total polymerization time = 180 s
Electrolyte : $LiClO_4$
Rotation rate : 1600 rpm

Table 3.4 Polymerization charges, cycling charges and coulombic efficiencies of polymerization for the polymer films prepared in the experiments of Figure 3.7

Curve No.	Rotation Rate ω (rpm)	Polymerization Charge $Q_{pol.}$ (mC)	Cycling Charge		Coulombic Efficiency	
			$Q_{ox.}$ (μC)	$Q_{red.}$ (μC)	from $Q_{ox.}/Q_{pol.}$ (%)	from $Q_{red.}/Q_{pol.}$ (%)
a	0	7.092	673.7	666.6	73.1	72.3
b	400	6.587	610.5	621.0	71.3	72.5
c	900	1.545	137.4	136.0	68.4	67.7
d	1600	0.945	81.7	79.9	66.5	65.0

Total polymerization time = 180 s
Electrolyte : Et_4NClO_4

In Tables 3.2 and 3.3, since the electrode rotation was started or stopped after a certain polymerization time, the total polymerization charge, the cycling charge and thus the coulombic efficiency are related to the proportion of time that the electrode was stationary (or rotating) during the polymerization period. In general, a longer stationary time provides more charge consumed for polymer formation, more polymer deposited on the electrode (*i.e.*, more cycling charges) and a higher coulombic efficiency, regardless of whether the electrode is rotating or not when the polymerization starts. A moderate decrease in the polymerization charge and the cycling charge is observed as the rotation time is prolonged, in contrast to that presented in Table 3.1 where much larger changes were observed when the electrode was rotated.

3.2.2.2 A.C. Impedance Studies

Impedance spectroscopy was applied to determine the ionic resistance of the resulting polymer films. A finite transmission line model[14,15] was used to interpret the impedance data obtained, as in earlier reports from this laboratory.[16] A.C. impedance responses (Nyquist plots) of the polymer films prepared in the experiments of Et_4NClO_4/acetonitrile solution are shown in Figure 3.11.

The plots shown in Figure 3.11 all consist of two distinct regions, approximating the behaviour of a finite transmission line.[14] At high frequency, linear regions with angles between 65° and 45° are observed, representative of the theoretical 45° Warburg-type region. Linear regions at nearly 90° appear at low frequency. By using the transmission line model, the resistance of the polymer film can be obtained either by analyzing data in the Warburg-type region or from the real impedance (Z') at low frequency.

An approach similar to that reported in the literature[16] was adopted. Only oxidized polymer films were analyzed here, the measured resistance is therefore the polymer's ionic resistance (R_I), since the electronic resistance (R_E) will be too small to measure. The capacitance (C) of each polymer film which was attributed to the oxidation and reduction of the polymer,[17,18] was calculated as the slope of a plot of imaginary impedance (Z'') vs. the reciprocal of frequency ($1/\omega$) from the low frequency region. The slope of an (impedance)^2 (Z^2) vs. the reciprocal of frequency ($1/\omega$) plot for the Warburg-type region provides R_I/C, from which the ionic resistance (R_I) can be obtained.

Figure 3.12 gives an example of the determination of capacitance (C) and

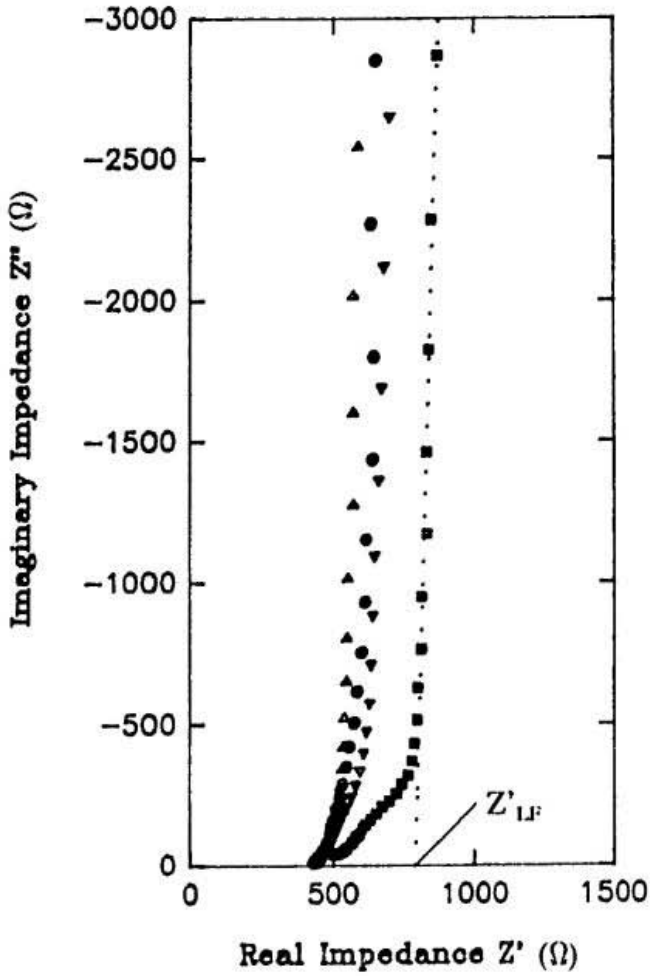

Figure 3.11 Impedance plots for the poly(3-methylthiophene) coated Pt electrodes prepared at (△) 0 rpm; (•) 400 rpm; (▽) 900 rpm and (■) 1600 rpm in the experiments of Figure 3.7. The experiments were carried out at 1.0 V in 0.1 M Et_4NClO_4/CH_3CN.

ionic resistance (R_I) for a polymer film prepared at 1600 rpm (Fig. 3.11d). It has to be mentioned that, although straight lines are presented in this case, slightly curved Z' vs. $1/\omega$ plots were observed when analyzing impedance data for all other films. The deviation from a linear relationship is thought to be related to the steeper Warburg-type region (*i.e.*, angles are greater than 45°) observed in those cases (Figure 3.11).

To estimate R_I from the low frequency region, the data was extrapolated as shown by the dotted line in Figure 3.11d for instance. Its intercept on the real impedance axis (*i.e.*, the limiting real impedance Z'_{LF}) was corrected by the uncompensated solution resistance (R_S) and then tripled to give the ionic resistance (R_I), since $R_I = 3(Z'_{LF} - R_S)$.[14] The uncompensated solution resistance (R_S) was obtained from the intercept at the real impedance axis of the Z'' vs. Z' plot for a bare Pt electrode.

Ionic resistances both from the Warburg-type region and from the low frequency data as well as capacitances are listed in Table 3.5. Ionic resistances measured by the two methods are in good agreement, and increase with increasing rotation rate during the polymerization. That is, the thinner polymer films

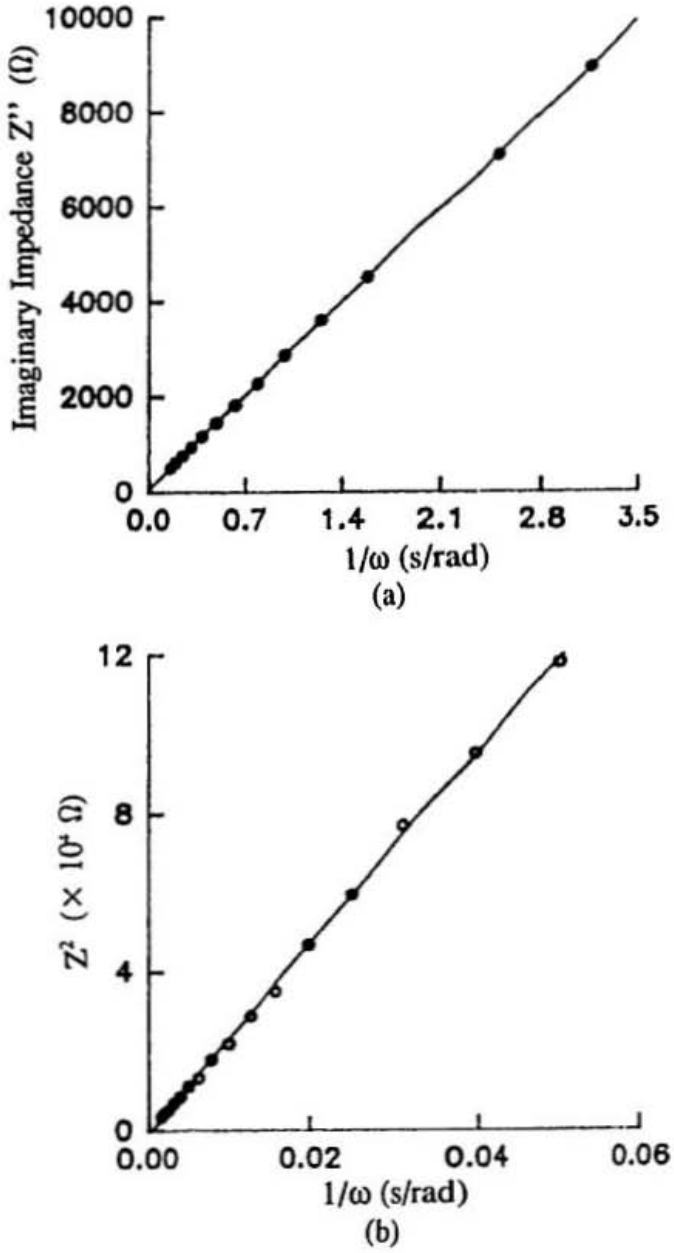

Figure 3.12 Plots for determination of (a) capacitance and (b) ionic resistance for a poly(3-methylthiophene) coated Pt electrode from impedance data shown in Figure 3.11(■).

Table 3.5 Capacitances and ionic resistances calculated from impedance data for the poly(3-methylthiophene) coated Pt electrodes prepared in the experiments Figure 3.7

Curve No.	Rotation Rate ω (rpm)	Capacitance C (μF)	Ionic Resistance (R_1)	
			Warburg Region (Ω)	from Z'_{LF} (Ω)
a	0	631.1	205	236
b	400	450.6	500	412
c	900	120.9	470	490
d	1600	56.6	853	899

consisting of less polymer exhibit higher resistance. However, the film capacitance which is proportional to the doping charge decreases with the increase in rotation rate.

3.2.3 Morphological Studies

In general, thick polymer films with a rough appearance were obtained at stationary electrodes, whereas thin compact polymer films could be obtained at high rotation rates. For example, the poly(3-methylthiophene) film prepared in the experiments of Figure 3.1a was matt black and looked porous, however the electrode surface was covered with a dark green, glossy and compact polymer film following the polymerization depicted in Figure 3.1c. Similar observations were made when the Et_4NClO_4/acetonitrile polymerization medium was used. A thick polymer film can still be prepared on a rapidly rotated disc electrode and usually has a pattern of hydrodynamic flow lines analogous to the classical spiral appearance based on rotating disc electrode theory,[9] in contrast to the disc-shaped coverage on the polymer-modified stationary electrode surface.

The morphology of the modified electrode surfaces was further probed by

scanning electron microscopy (SEM). Reduced polymer films prepared via potential steps for 3 min. were rinsed with acetone prior to examination. As can be seen in Figure 3.13, the heterogeneous poly(3-methylthiophene) film on the stationary electrode consists of polymeric aggregates (Figure 3.13b) and fibrillar structures (Figure 3.13c), located randomly on the electrode surface (Figure 3.13a). The appearance of polymer films produced at high rotation rates is significantly different. Uniform surfaces were obtained at rotation rates of 900 rpm (Fig. 3.15) and 1600 rpm (Fig. 3.16), especially at 1600 rpm where a compact surface is observed (Fig. 3.16c).

In comparison with the film on the stationary electrode (Fig. 3.13), the film prepared at 400 rpm is more homogeneous (Fig 3.14), although the amount of polymer precipitated is quite similar as demonstrated in Table 3.4. No fibrillar structure is observed, but there is a large accumulation of polymer aggregates unevenly distributed on the surface, which were absent at higher rotation rates (Fig 3.15 and 3.16).

The thickness of the grafted polymer film as well as the nature of the monomer, the nature of the anion and the degree of doping influence the

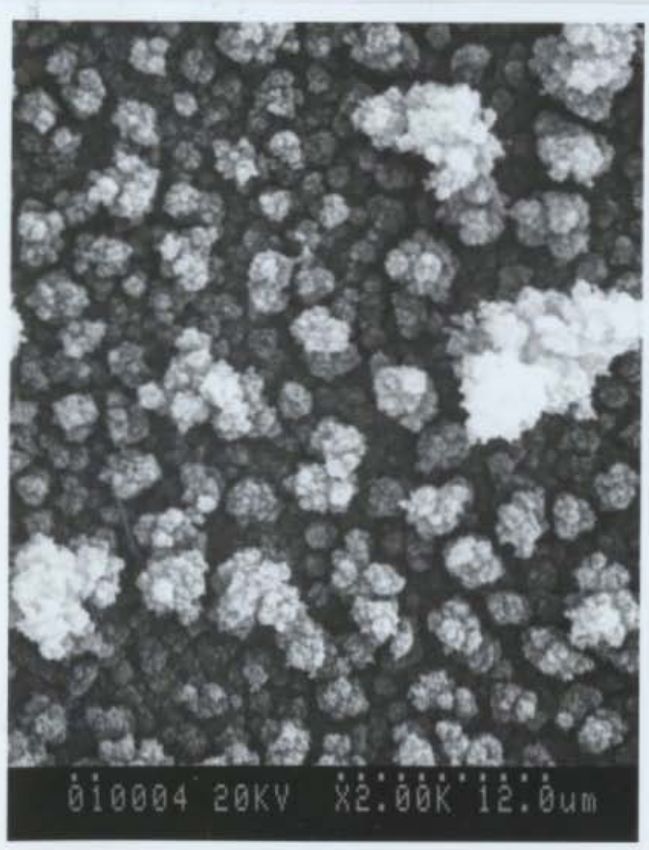

Figure 3.13 Scanning electron micrographs for the polymer film prepared on a stationary electrode as shown in Figure 3.7a. Polymerization time: 3 min.

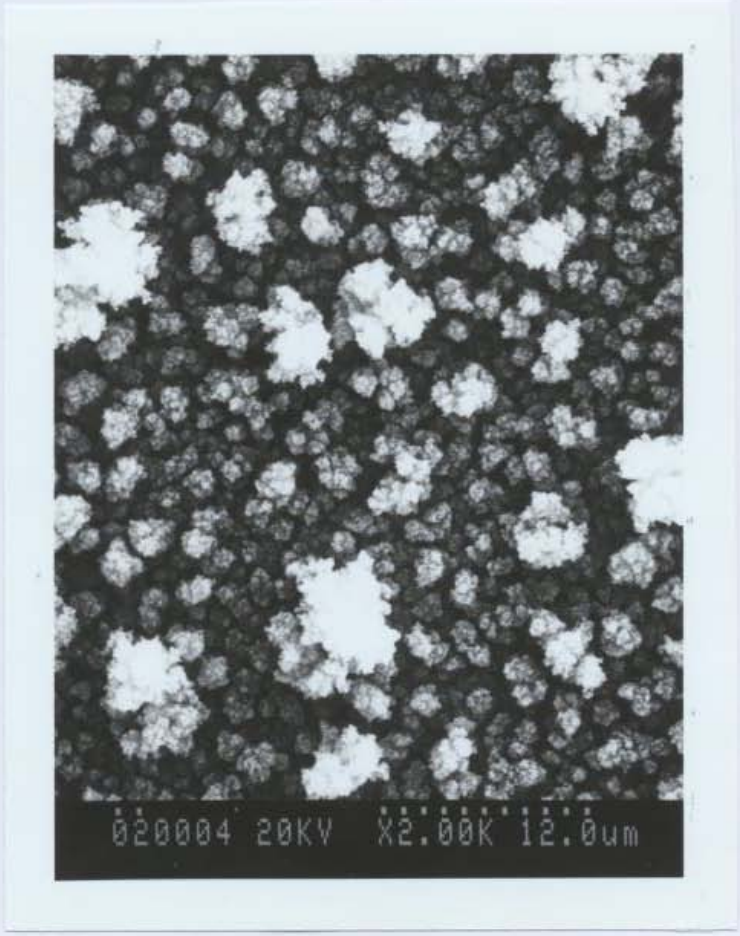

Figure 3.14 Scanning electron micrographs for the polymer film prepared on a rotating electrode at 400 rpm as shown in Figure 3.7b. Polymerization time: 3 min.

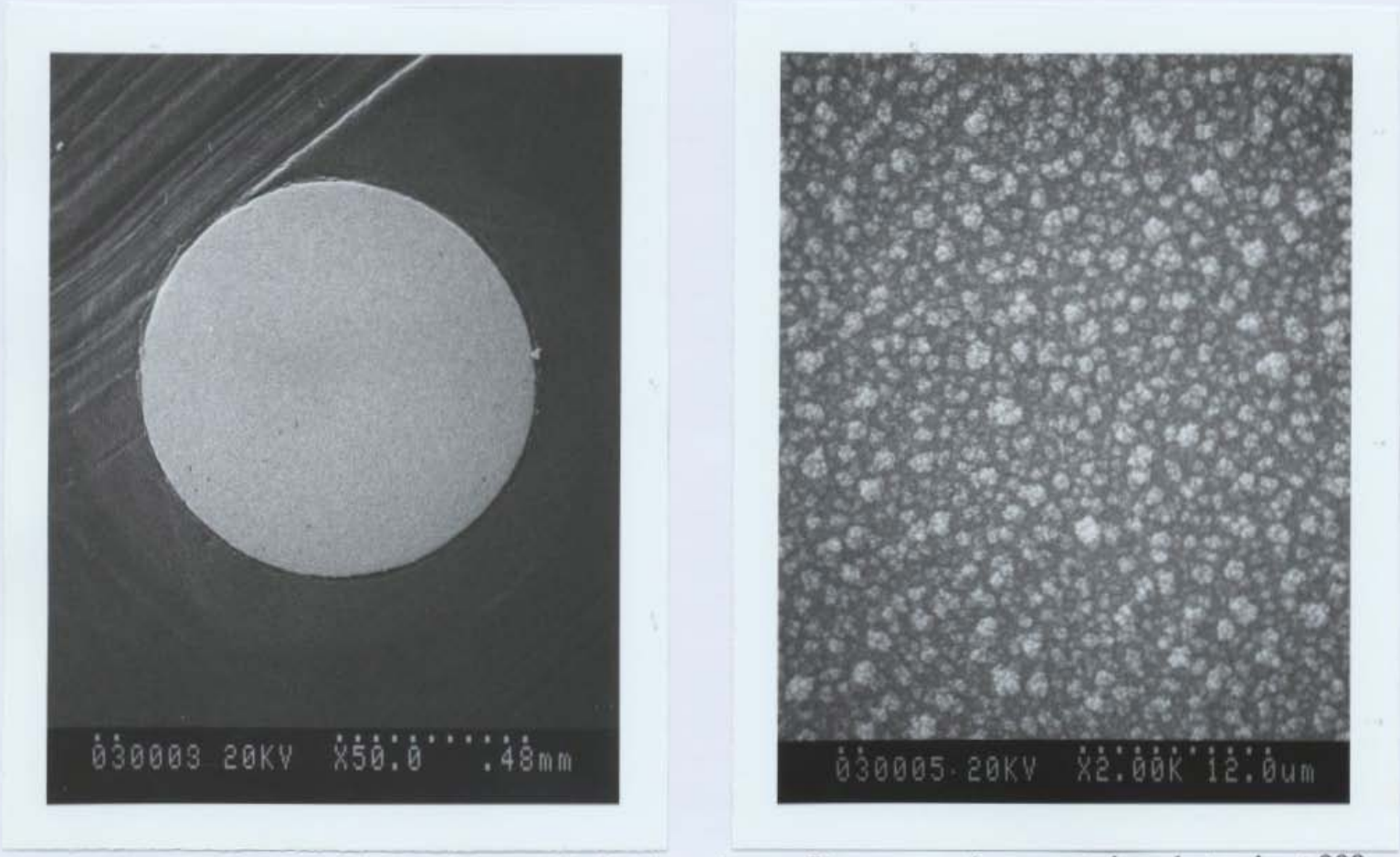

Figure 3.15 Scanning electron micrographs for the polymer film prepared on a rotating electrode at 900 rpm as shown in Figure 3.7c. Polymerization time: 3 min.

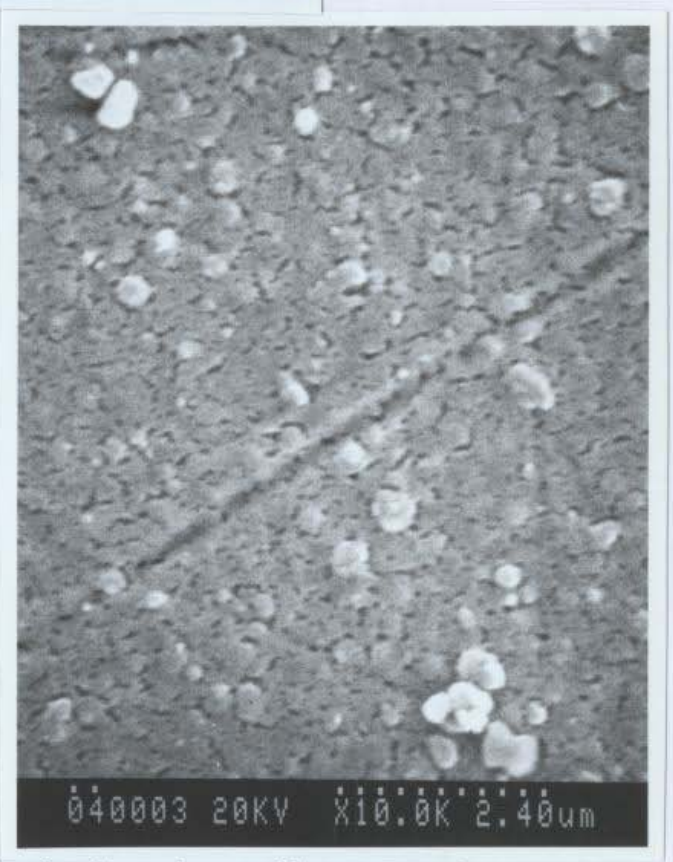

Figure 3.16 Scanning electron micrographs for the polymer film prepared on a rotating electrode at 1600 rpm as shown in Figure 3.7d. Polymerization time: 3 min.

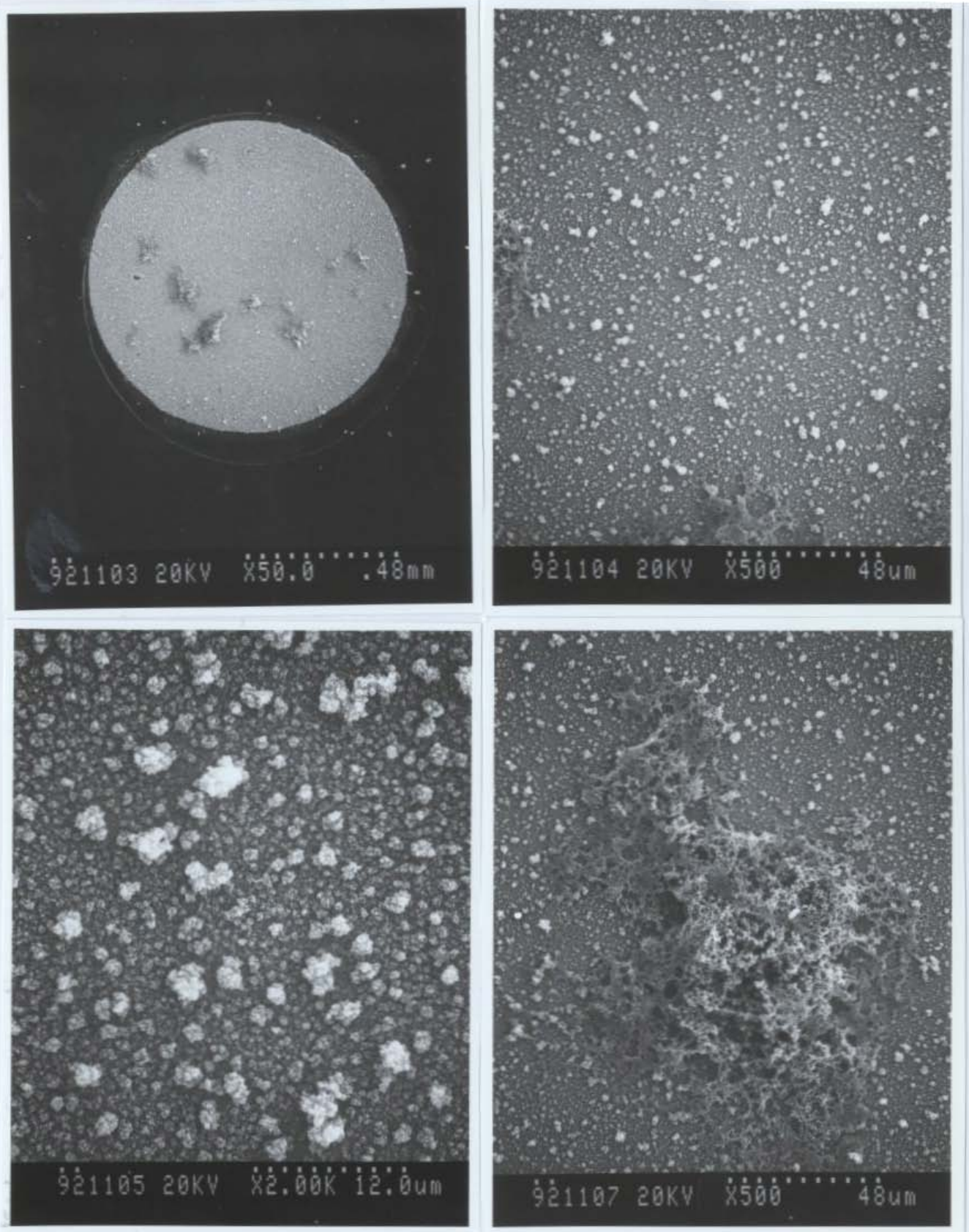

Figure 3.17 Scanning electron micrographs for the polymer film prepared on a stationary electrode under the experimental conditions as shown in Figure 3.7, but the polymerization time was 1.5 min.

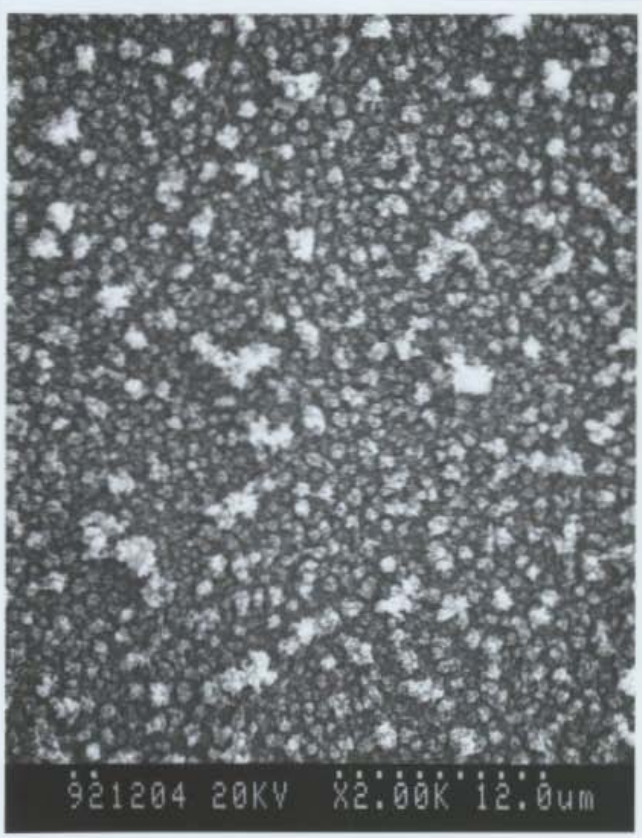

Figure 3.18 Scanning electron micrographs for the polymer film prepared on a rotating electrode at 400 rpm under the experimental conditions as shown in Figure 3.7, but the polymerization time was 1.5 min.

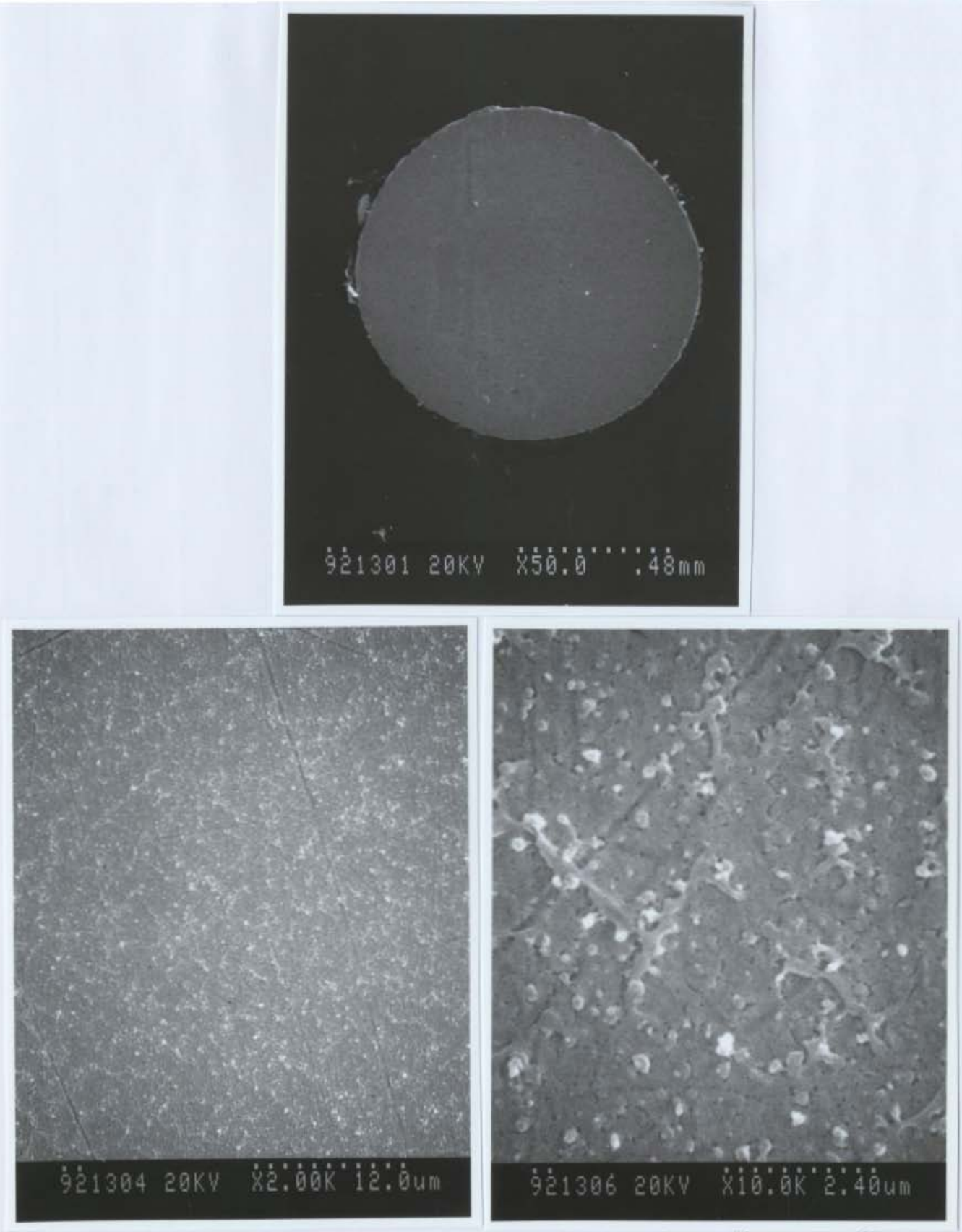

Figure 3.19 Scanning electron micrographs for the polymer film prepared on a rotating electrode at 900 rpm under the experimental conditions as shown in Figure 3.7, but the polymerization time was 1.5 min.

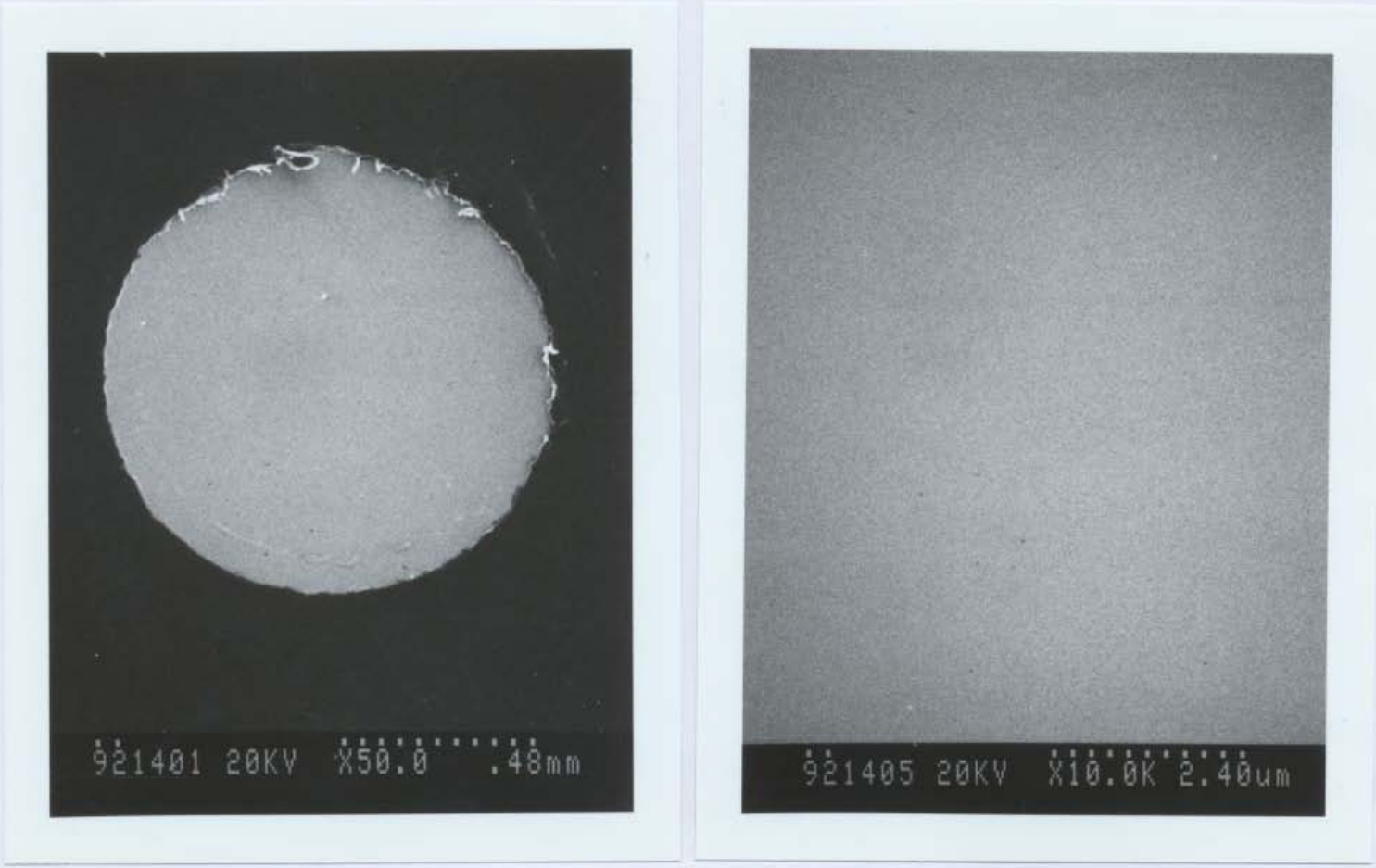

Figure 3.20 Scanning electron micrographs for the polymer film prepared on a rotating electrode at 1600 rpm under the experimental conditions as shown in Figure 3.7, but the polymerization time was 1.5 min.

morphology of the polymer deposited.[26] To investigate the dependence of morphology on thickness, poly(3-methylthiophene) films prepared for only 1.5 min. using the same potential steps were examined by SEM. As shown in Figure 3.17, despite the lower amount of polymer deposited compared with Figure 3.13 and 3.14, and the more homogeneous appearance of the film (*i.e.*, comparing Fig. 3.17a with Fig. 3.13a), aggregates and fibrillar structures were still observed on the surface of a stationary electrode (Fig. 3.17c). When the electrode was rotated and particularly at high rotation rates, the surface of the resulting polymer films becomes uniform and compact, as presented in Figure 3.18 and 3.19 at rotation rates of 400 rpm and 900 rpm, respectively. A very smooth polymer surface was obtained on a rotating electrode at 1600 rpm (Fig. 3.20).

3.3 Discussion

The main mechanisms that have been proposed for the growth and deposition of poly(3-methylthiophene) can be summarized by the following simple equations, where the subscripts (sol.) and (surf.) represent species in solution and on the electrode surface, respectively. The first step of the polymerization involves

the oxidation of the monomer to provide a radical cation:

$$MeTh \rightarrow MeTh^{+\bullet} + e^-$$

The following processes for oligomer formation consist of the reaction of a monomeric species with a monomeric or oligomeric radical, which may occur (a) on the electrode surface or (b) in the reaction layer close to the electrode surface:

(a) $(MeTh)_n^{+\bullet}{}_{(surf.)} + MeTh^{+\bullet}{}_{(sol.)} \rightarrow (MeTh)_{n+1(surf.)} + 2H^+$

or $(MeTh)_n^{+\bullet}{}_{(surf.)} + MeTh_{(sol.)} \rightarrow (MeTh)_{n+1(surf.)} + 2H^+ + e^-$

(b) $(MeTh)_n^{+\bullet}{}_{(sol.)} + MeTh^{+\bullet}{}_{(sol.)} \rightarrow (MeTh)_{n+1(sol.)} + 2H^+$

or $(MeTh)_n^{+\bullet}{}_{(sol.)} + MeTh_{(sol.)} \rightarrow (MeTh)_{n+1(sol.)} + 2H^+ + e^-$

As the polymerization proceeds, oligomers produced from route (b) may either precipitate on the electrode surface when they reach a critical chain length, or be transported to the bulk solution by diffusion/convection.

As discussed in Section 3.2.1, the current at long times (or $t > 25$ s) in the *I-t* transients decreases with increasing rotation rate and prolonging rotation time during polymerization. If the rising current at $t > 25$ s for a stationary electrode (*e.g.*, Fig. 3.1) arises only from the oxidation of the monomer, an increasing current would have been observed as the rotation rate was increased, due to the faster monomer transport from the bulk solution, and thus the higher monomer

concentration in the diffusion layer. However, the experimental observation is contrary to this expectation. It is therefore concluded that the rising current in the chronoamperometric transient after ca. 25 s of polymerization at a stationary electrode is due to the oxidation of oligomeric species in the vicinity of the electrode. The accumulation of such species accounts for the current increase with time, while their dispersion accounts for the decreasing current with increasing rotation rate.

The coulombic efficiency for the polymerization decreases at increasing rotation rates and at prolonged rotation times during polymerization (Tables 3.1 to 3.4). This behaviour supports the conclusion that soluble oligomeric intermediates are formed in the diffusion layer during the polymerization and that these oligomeric species contribute to polymer deposition, especially at a stationary electrode where the highest coulombic efficiency was obtained. When the electrode is rotated, the diffusion layer becomes thinner and the concentration of oligomers in the vicinity of the electrode decreases owing to forced convection. As a result, polymerization occurs less effectively and produces less polymer on the electrode surface than on a stationary electrode, as evidenced by the cycling charges and coulombic efficiencies.

The morphology of the polymer film deposited changes when the electrode is rotated. As shown by the photographs in Section 3.2.3, both heterogeneous and homogeneous film appearances were observed. An acceptable interpretation for the experimental observations is that the loose fibrillar/aggregate structure results from the precipitation of oligomeric intermediates from the solution, while the compact uniform film arises from the addition of monomeric species into the polymer matrix.

Differences in the early stages of polymerization between stationary and rotating electrodes were also observed. Compared with a rotating electrode, less time is required both for the decay of the initial spike and for the initial rising *i-t* transient at a stationary electrode. This indicates a decrease in the rate of nucleation and growth on a rotating electrode and can be attributed to the enhanced transport of soluble oligomeric intermediates away from the electrode prior to precipitation. Therefore, nucleation and progressive polymerization appears to involve oligomers generated in solution. At a rotating electrode, the concentration of soluble oligomers decreases. As a result, a longer time is required for the early stages of polymerization at a rotating electrode.

In Figure 3.3, a drop in current was observed when the electrode started rotating during polymerization, indicating loss of electroactive sites in the reaction layer near the electrode due to stirring. Therefore, the recorded *i-t* transient at the moment of rotation results from the superposition of the loss of oligomers in the solution with further polymer growth mainly involving the reaction of the polymer matrix with the increased amount of monomeric species.

Impedance data showed that the ionic resistance of the polymer film deposited increases with increasing rotation rate, which is consistent with the morphological evidence discussed above. It is reasonable that films with a dense structure like the film in Figure 3.16 should possess a higher ionic resistance than a loose film (*e.g.*, Fig. 3.13) despite being much thinner.

As a conclusion, polymer deposition may take place both through soluble oligomers in the reaction layer and via the grafted polymer matrix on the electrode surface. Each process can dominate polymer growth under certain conditions. At a stationary electrode, due to the presence of a thick diffusion layer, soluble oligomeric species build up in the vicinity of the electrode, and eventually precipitate on the electrode surface when the solubility decreases as the chains

propagate. Meanwhile, progressive addition of monomer or monomeric radical cation to the ends of polymer chains in the deposited film will also occur, contributing to the polymer formation. From the experimental data and the above discussion, it appears that the polymerization process mainly occurs via the precipitation of oligomeric chains from solution, at least at times longer than ca. 25 s.

There are drastic changes when the electrode rotates. Not only is the diffusion layer close to the electrode thinner, but also the oligomer concentration in the vicinity of the electrode decreases owing to convection, and more monomer is brought to the electrode surface. The monomer may react with the polymer chain ends directly or be oxidized to give a radical cation. The resulting radical cation may couple with polymer chains on the surface, or be transported to the bulk solution by the stirring, or form soluble short chain oligomers which may also be removed away from the vicinity of the electrode by convection. The latter two processes together with the decrease in oligomer concentration account for the decrease in coulombic efficiency with rotation (Tables 3.1 to 3.4). It is therefore concluded that polymer formation is dominated by reactions involving the grafted polymer matrix at high rotation rates.

3.4 Conclusion

Conducting polymer films of poly(3-methylthiophene) have been electrochemically deposited both on stationary and rotating disc electrodes via the potential step technique. Poly(3-methylthiophene) films can be formed even at a rotation rate as high as 1600 rpm, in contrast to some prior reports[21,22] where no polymer film deposition was observed on rotating electrodes.

It appears that polymer deposition takes place through two simultaneous processes, that is, polymer chain propagation occurs both at the ends of polymer chains in the polymer matrix and via soluble oligomeric species which eventually precipitate on the electrode surface. The precipitation of oligomeric species with a critical chain length dominates polymer deposition on a stationary electrode particularly at long times, whereas the grafting of monomeric species onto polymer chains deposited on the electrode surface dominates polymer growth when the electrode is rotated at 1600 rpm.

Polymer films were characterized by cyclic voltammetry, impedance spectroscopy and scanning electron microscopy (SEM). The charge consumed

during polymerization and the charge observed in cyclic voltammetry were integrated to provide the coulombic efficiency which was found to be decreased by rotation (Table 3.1 to 3.4). SEM studies revealed substantial morphological differences between polymer films prepared under various conditions. A porous matt surface was observed for films deposited on a stationary electrode, whereas compact smooth films were obtained at high rotation rates. Thus improved surface homogeneity of the resulting polymer films is obtained by rotating the electrode. A.C. impedance spectroscopy showed that polymer films with higher resistances and lower capacitances were produced as the electrode rotation rate was increased.

By monitoring the current-time responses, the polymerization was investigated at various rotation rates, by beginning or halting rotation at different times during polymer formation, at different oxidation potentials and in two different electrolyte solutions. In general, less polymer was deposited at higher rotation rates (Fig. 3.1 and 3.7), and when the rotation time during polymerization was longer (Fig. 3.3 and 3.4). This was interpreted as conclusive evidence that the polymerization involves the formation of oligomers in solution.

References

1. K. Tanaka, T. Shichiri, S. Wang, and T. Yamabe, *Synth. Met.*, 1988, **24**, 203.

2. D.E. Raymond and D.J. Harrison, *J. Electroanal. Chem.*, 1990, **296**, 269.

3. S. Bruckenstein and J.W. Sharkey, *J. Electroanal. Chem.*, 1988, **241**, 211.

4. P. Lang, F. Chao, M. Costa, E. Lheritier, and F. Garnier, *Ber. Bunsenges. Phys. Chem.*, 1988, **92**, 1528.

5. Y. Wei, C.-C. Chan, J. Tian, G.-W. Jang, and K.F. Hsueh, *Chem. Mater.*, 1991, **3**, 888.

6. S. Asavapiriyanont, G.K. Chandler, G.A. Gunawardena, and D. Pletcher, *J. Electroanal. Chem.*, 1984, **177**, 229.

7. A.R. Hillman and E.F. Mallen, *J. Electroanal. Chem.*, 1987, **220**, 351.

8. B.R. Scharifker, E. Garciapastoriza, and W. Marino, *J. Electroanal. Chem.*, 1991, **300**, 85.

9. J.A. Harrison and H.R. Thirsk, in *Electroanalytical Chemistry*, vol. 3, A.J. Bard, Ed. (Marcel Dekker, New York, 1971), p. 67.

10. F.B. Li and W.J. Albery, *Electrochimica Acta*, 1992, **37**, 393.

11. R. John and G.G. Wallace, *Polymer International*, 1992, **27**, 255.

12. A.J. Downard and D. Pletcher, *J. Electroanal. Chem.*, 1986, **206**, 147.

13. T.F. Otero, C. Santamaria, E. Angulo, and J. Rodriguez, *Synth. Met.*, 1991, **43**, 2947.

14. W.J. Albery, C.M. Elliott, and A.R. Mount, *J. Electroanal. Chem.*, 1990, **288**, 15.

15. X. Ren and P.G. Pickup, *J. Chem. Soc., Faraday. Trans.*, 1993, **89**, 321.

16. G.L. Duffitt and P.G. Pickup, *J. Chem. Soc., Faraday. Trans.*, 1992, **88**, 1417.

17. J. Heinze, *Synth. Met.*, 1991, **41-43**, 2805.

18. M. Kalaji and L.M. Peter, *J. Chem. Soc., Faraday. Trans.*, 1991, **87**, 853.

19. A.J. Bard and L.R. Faulkner, Eds., *Electrochemical Methods: Fundamentals and Applications* (John Wiley and Sons Inc.,, 1980).

20. A.F. Diaz and J. Bargon, in *Handbook of Conducting Polymers*, vol. 1, T.A. Skotheim, Ed. (Marcel Dekker: New York,, 1986), pp. 81-115.

21. R. John and G.G. Wallace, *J. Electroanal. Chem.*, 1991, **306**, 157.

22. L.L. Miller, B. Zinger, and Q.-X. Zhou, *J. Am. Chem. Soc.*, 1987, **109**, 2267.

Chapter 4

Electrochemical Synthesis of Poiy(3-Bromothiophene) in the Presence of 2,2'-Bithiophene

4.1 Introduction

In the last few decades, increasing interest has developed in the preparation of modified electrodes from conducting polymers. Among these, polymers of thiophene derivatives have been vigorously investigated in view of the fact that substituents on the monomer influence significantly the properties of the resulting polymer, some of which are capable of electrocatalysis or molecular recognition.[1] Although many tailor-made, functionalized monomers can be directly electropolymerized, the steric effects of large functional groups can prevent the formation of polymers with good electronic and electrochemical properties. Poly(3-bromothiophene) is an attractive material for further modification into useful functionalized polymers, since the bromo- leaving groups are potential sites for introduction of desired substituents.

Initially mentioned by Waltman *et al.*,[4] the electrochemical synthesis of poly(3-bromothiophene) was found to be difficult, requiring a much higher oxidation potential than for thiophene or 3-alkylthiophenes due to the electron withdrawing effect of the bromine on the electron density of the thiophene ring. Although optimization of the electrosynthetic conditions to produce highly conducting films has been investigated,[5] and microscopic studies of the surface and electronic structure of the polymer have also been reported,[6,7] poly(3-bromothiophene) has received far less attention than polymers from many other thiophene-based monomers.

Thin conducting polymer films of 3-bromothiophene can be obtained adhering to the working electrode by electrochemical polymerization.[8] However, a colour change in the solution near the electrode surface is observed during film growth, and coloured species diffuse into the bulk solution in long-time experiments. It was assumed that this is because highly soluble oligomers and short-chain polymers are formed, which are stable enough to diffuse away from the electrode. The chain propagation may be obstructed by steric hindrance due to the bulky bromo- substituent.[4]

As reported by Garnier and co-workers,[5] the electrodeposition of poly(3-bromothiophene) is much slower than for polythiophene, both in cyclic voltammetry and potentiostatic polymerization. The steric effect of the bromo-substituents results in a torsion angle between adjacent monomer units, which in turn leads to a loss of inter-ring conjugation.[4,8] It was suggested that the lower polymerization rate in the case of 3-bromothiophene is due to the less conjugated structure of the polymer which results in less efficient charge transfer during film deposition.[5]

An improved method for the preparation of electrically conductive polymers of thiophene and 3-alkylthiophenes has been recently reported by Wei's group.[9,10] Adding a small amount of 2,2'-bithiophene or 2,2':5',2''-terthiophene to the monomer solution produces a pronounced increase in the rate of polymerization and some decrease in the required oxidation potential. It was presumed that in the presence of the additives, the number of nuclei for polymer formation is much greater, leading to faster polymerization and more uniform polymer films. Similar results have also been reported on the polymerization of aniline and alkyl ring-substituted anilines by the same group.[11] Dramatically increased rates of polyaniline formation were achieved in the presence of additives such as *p*-

aminodiphenylamine, benzidine and *p*-phenoxyaniline.

Interestingly, Wei and co-workers found that only poly(3-methylthiophene) was produced from a mixed monomer solution containing 0.2 mM bithiophene and 0.2 M 3-methylthiophene, even under conditions where more polymer could be prepared from 0.2 mM bithiophene alone than from 0.2 M 3-methylthiophene alone.[10] Electrochemical and infrared spectroscopic studies on the polymers prepared revealed no structural differences between poly(3-methylthiophene) films synthesized in the presence and absence of bithiophene. Thus, although a copolymer of bithiophene and methylthiophene would intuitively be expected, it appears that the bithiophene acts predominantly as a catalyst for electrochemical deposition of 3-methylthiophene. However, the mechanism of the polymerization in the presence of bithiophene is still not well understood.

To further investigate the role of a catalytic amount of bithiophene in the process of polymer growth and thus the mechanism of polymer generation, and to demonstrate the facility of the new synthetic method for efficient polymerization for more systems, electrically conductive poly(3-bromothiophene) has been prepared by applying this method. Polymers generated were characterized by x-ray

emission spectroscopic microanalysis as well as by cyclic voltammetry. Polymer formation and characterization will be discussed in the following sections in detail. The kinetics of the polymerization and the mechanism will be discussed in Chapter 5.

4.2 Results

4.2.1 Electrochemical Polymerization

As mentioned above, poly(3-bromothiophene) can be prepared by electrochemical polymerization of the 3-bromothiophene monomer. Either potentiostatic or cyclic voltammetry techniques may be utilized and high oxidation potentials (ca. >1.8 V vs. SSCE) are required to obtain an acceptable rate of polymer growth. One of the disadvantages of the use of high oxidation potentials is the occurrence of simultaneous side reactions, such as mislinkage, crosslinking and degradation of the polymer, resulting in a poor quality film.[12,13] Kinetic studies have suggested that the rate-determining step in the polymerization of thiophenes is usually the initial oxidation of the monomer. Subsequent oxidation of the dimeric

intermediate is much faster, and can take place at a lower oxidation potential than for the monomer.[14,15] Therefore, we introduced a small amount of a dimeric species (i.e., 2,2'-bithiophene) into the bromothiophene polymerization system, seeking to avoid the slow initial step, to reduce the required oxidation potential and to increase the overall rate of polymerization.

Typical cyclic voltammograms for the electrochemical polymerization of 0.2 M bromothiophene in 0.1 M Bu_4NPF_6/acetonitrile solutions are shown in Figure 4.1. The potential was cycled through the potential range of -0.2 to 1.95 V vs. SSCE at a scan rate of 100 mV/s. Figure 4.1a shows the polymerization of bromothiophene in the absence of bithiophene. In the first scan no oxidation is observed until ca. 1.80 V. But the current in the reverse scan is higher than in the forward scan over the potential range positive of 1.65 V. This nucleation loop is a common observation where a new phase is formed by a nucleation and growth mechanism.[16] The irreversible oxidation peak shows that the intermediate radical cation is extremely reactive and unstable. This oxidation leads to the formation of a thin polymeric film on the electrode surface, as evidenced by the broad reduction peak covering the potential range between 0.65 and 1.65 V, and by the oxidation peak commencing at 1.1 V in the second cycle. An anodic peak at ca. 1.35 V vs.

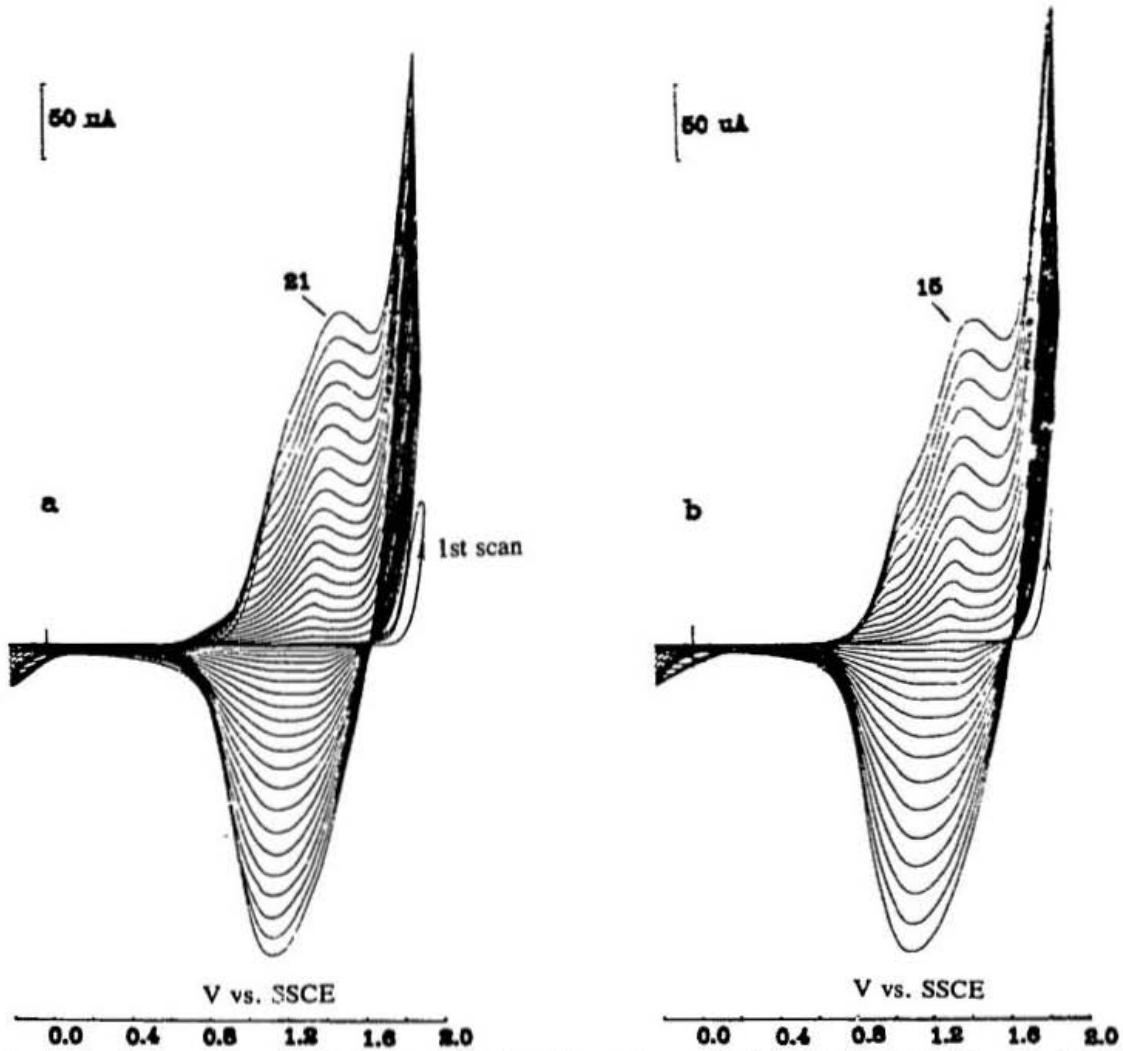

Figure 4.1 Cyclic voltammograms at 100 mV/s for the polymerization of 0.2 M 3-bromothiophene in 0.1 M Bu_4NPF_6/CH_3CN (a) in the absence and (b) in the presence of 0.2 mM 2,2'-bithiophene.

SSCE appears in the subsequent scans, corresponding to the oxidation of poly(3-bromothiophene). The anodic peaks shift gradually to higher potential as the polymerization proceeds, which is attributed to the increasing resistance of the polymer film.[17,18] The peak currents increase in successive scans, indicating the growth of polymer on the electrode.

Introducing a small amount of bithiophene into the monomer solution produces a new anodic peak at ca. 1.25 V in the first potential scan (Fig. 4.1b). This is obviously due to the oxidation of bithiophene. It was confirmed by cyclic voltammograms for bithiophene polymerization in the absence of bromothiophene, in which the anodic peak for the oxidation of bithiophene was observed at ca. 1.25 V. At higher potentials in the bromothiophene/bithiophene system, the sharp increase in the anodic current is due to the oxidation of bromothiophene. As in Figure 4.1a, a nucleation loop appears, followed by a broad reduction peak in the reverse scan. Oxidation of the polymer produced can be observed at ca. 1.35 V in the second and subsequent scans, and the onset of the anodic peak for polymer formation shifts to lower potentials. Only one reduction process is observed that is electrochemically reversible with a cathodic peak at ca. 1.20 V, comparable with that of the bithiophene-free system. Comparing Figure 4.1b with Figure 4.1a, it is

clear that with the addition of bithiophene, the rate of increase of the peak currents is significantly enhanced. With presence of bithiophene, fewer scans were required to reach a certain anodic peak current for polymer oxidation, *e.g.*, 15 scans shown in Figure 4.1b vs. 21 scans in Figure 4.1a, showing a faster polymer growth rate. Moreover, a smaller potential shift of the polymer oxidation peak is observed in the presence of bithiophene, suggesting that a polymer film with lower resistance is produced.

Both the anodic and the cathodic charges in a cyclic voltammogram of a polymer coated electrode are related to the amount of electroactive material grafted onto the surface of the electrode. However, the anodic scans recorded during polymer growth are more complicated than the corresponding cathodic scans because they involve both the oxidation of the polymer deposited on the electrode and the formation of new polymer. It is only the charge consumed in the redox processes of the polymer that is proportional to the amount of electroactive polymer and is useful for quantitative analysis. For example, the cathodic charge (Q_c) is due solely to the reduction of polymer on the surface of the electrode and is therefore proportional to the amount of polymer produced.[18,19] For this reason, cathodic charges recorded continuously during polymerization under potential cycling

conditions were used as a quantitative measures of the polymerization rate. The program named QT (see Section 2.2.1) was used to record the total cathodic charge vs. scan number, which represents the reaction time (t).

As shown in Figure 4.2, a plot of cathodic charge vs. scan number recorded during polymer formation from bromothiophene in the presence of bithiophene (Fig. 4.2c) is steeper than that for the bithiophene-free system (Fig. 4.2b). No significant generation of poly(2,2'-bithiophene) is observed from a pure bithiophene solution in the potential range of -0.2 to 1.9 V (Fig. 4.2a), probably because any polymer that is formed is deactivated by overoxidation at the high positive potential.[20-22] Apparently, the enhanced cathodic charge of each scan in Figure 4.2c is not simply a sum of the corresponding cathodic charges for poly(3-bromothiophene) and poly(2,2'-bithiophene), indicating that the increased rate of polymerization does not arise from simultaneous deposition of both poly(2,2'-bithiophene) and poly(3-bromothiophene).

The rate of polymer growth defined as dQ_c/ds can be represented by the slope of the cathodic charge (Q_c) vs. scan number (s) plot after the induction period. Calculated from the plots in Figure 4.2, the rate of polymer growth in the

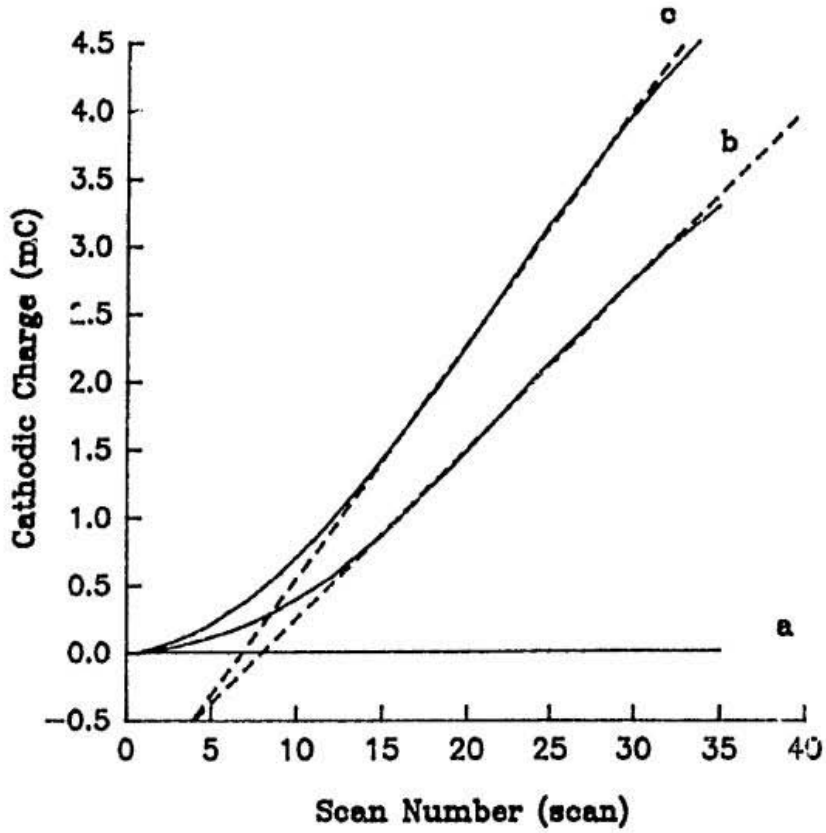

Figure 4.2 Plots of cathodic charge against scan number for the polymerization of (a) 0.2 mM 2,2'-bithiophene; (b) 0.2 M 3-bromothiophene and (c) 0.2 M 3-bromothiophene in the presence of 0.2 mM 2,2'-bithiophene. Potential range: -0.2 to 1.90 V. Scan rate: 50 mV/s.

absence of bithiophene (Fig. 4.2b) is 125 μC per scan, whereas a rate of 172 μC per scan was obtained when bithiophene was added to the solution (Fig. 4.2c). The potential cycling range was in every case -0.2 to 1.90 V at a scan rate of 50 mV/s. Repeating experiments under the same conditions gave average slopes of 172±4 μC/scan (4 experiments) for the bromothiophene/bithiophene system and 128±3 μC/scan (4 experiments) when bithiophene was absent, so that the polymerization rate of bromothiophene in the presence of bithiophene is ca. 1.34 times that in the absence of bithiophene.

To investigate the possibility that a lower oxidation potential is required for the polymerization of 3-bromothiophene in the presence of bithiophene, experiments were performed by sweeping to different oxidation potential limits, in the presence and absence of bithiophene. Experimental data showed that the bithiophene decreased the oxidation potential required by ca. 80 mV. For example, Figure 4.3 presents plots of cathodic charge against scan number when an upper potential limit of only 1.80 V was applied. In the absence of bithiophene (Fig. 4.3a), no significant cathodic charge could be measured and no polymer was produced even after 50 scans (ca. 1 h). However, the polymer was generated efficiently when only a small amount of bithiophene was added (Fig. 4.3b).

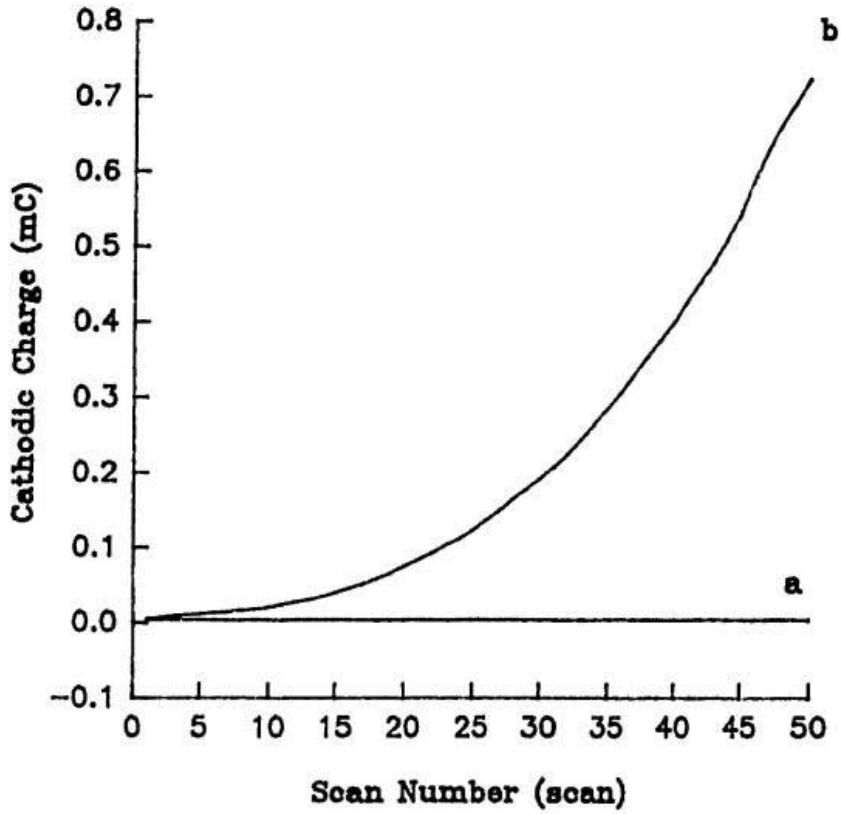

Figure 4.3 Plots of cathodic charge against scan number for the polymerization of 0.2 M 3-bromothiophene (a) in the absence and (b) in the presence of 0.2 mM 2,2'-bithiophene. Potential range: -0.2 to 1.80 V. Scan rate: 50 mV/s.

Further insight into the rate enhancement and the low polymerization potential required in the presence of bithiophene can be obtained by examining the induction periods seen in the plots of cathodic charge vs. scan number. It was found that before the polymer growth reaches a fast steady rate, an induction period is observed, in which the cathodic charge increases only slowly in the early stages of the polymerization (Fig. 4.2). Figure 4.4 shows the induction periods for the polymerization of bromothiophene using an upper potential limit of only 1.85 V in the presence and absence of bithiophene. The length of the induction period may be represented by the number of scans, obtained as shown in the figure. Clearly, in the absence of bithiophene (Fig. 4.4a), the induction period of about 35 scans is much longer than when an upper potential limit of 1.90 V (Fig. 4.2b) was used. Moreover, it decreased dramatically to only ca. 10 scans in the presence of bithiophene (Fig. 4.4b).

4.2.2 Morphology

The appearance of poly(3-bromothiophene) films prepared in the presence of bithiophene is comparable with those produced in the absence of bithiophene. In both cases, shiny compact polymer films were produced in the first few scans,

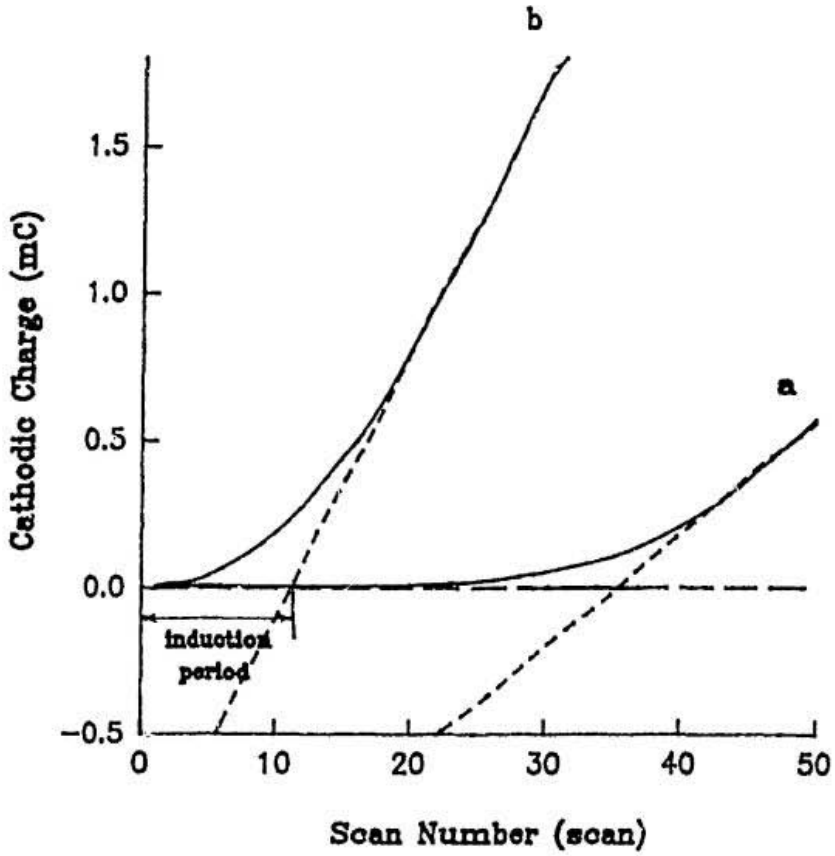

Figure 4.4 Plots of cathodic charge against scan number for the polymerization of 0.2 M 3-bromothiophene (a) in the absence and (b) in the presence of 0.2 mM 2,2'-bithiophene. Potential range: -0.2 to 1.85 V. Scan rate: 50 mV/s.

and the colour of the polymer changed from reddish brown (neutral) to black (oxidized) while it was cycled between its neutral and oxidized states. Films became matt black as the polymerization proceeded (> 5 scans) and expanded onto the insulating (PTFE) surface around the electrode. Scanning electron micrographs (SEM) for poly(3-bromothiophene) prepared in the presence of bithiophene (Fig. 4.5) reveal that the solution-side surface of a neutral polymer film deposited using 40 scans under the condition specified in Figure 4.2c is porous rather than smooth. Clusters of spherical polymeric lumps appear to have been deposited on the electrode surface at random with an amount of empty space.

The inhomogeneous morphology typified by Figure 4.5 was found to be more rapidly reached compared with the polymerization of poly(3-methylthiophene) (Section 3.2.3). Furthermore, poly(3-bromothiophene) films display a much more loosely packed and rougher surface (Fig. 4.5), and no fibrillar structure could be resolved. The accumulation of polymer aggregates in the poly(3-methylthiophene) coated electrodes is relatively greater. This is probably due to steric crowding[1] which hinders chain propagation and leads to a less planar polymer film of 3-methylthiophene. At scan numbers greater than ca. 30 scans during cyclic voltammetry, the solution became yellowish brown near the Pt electrode surface.

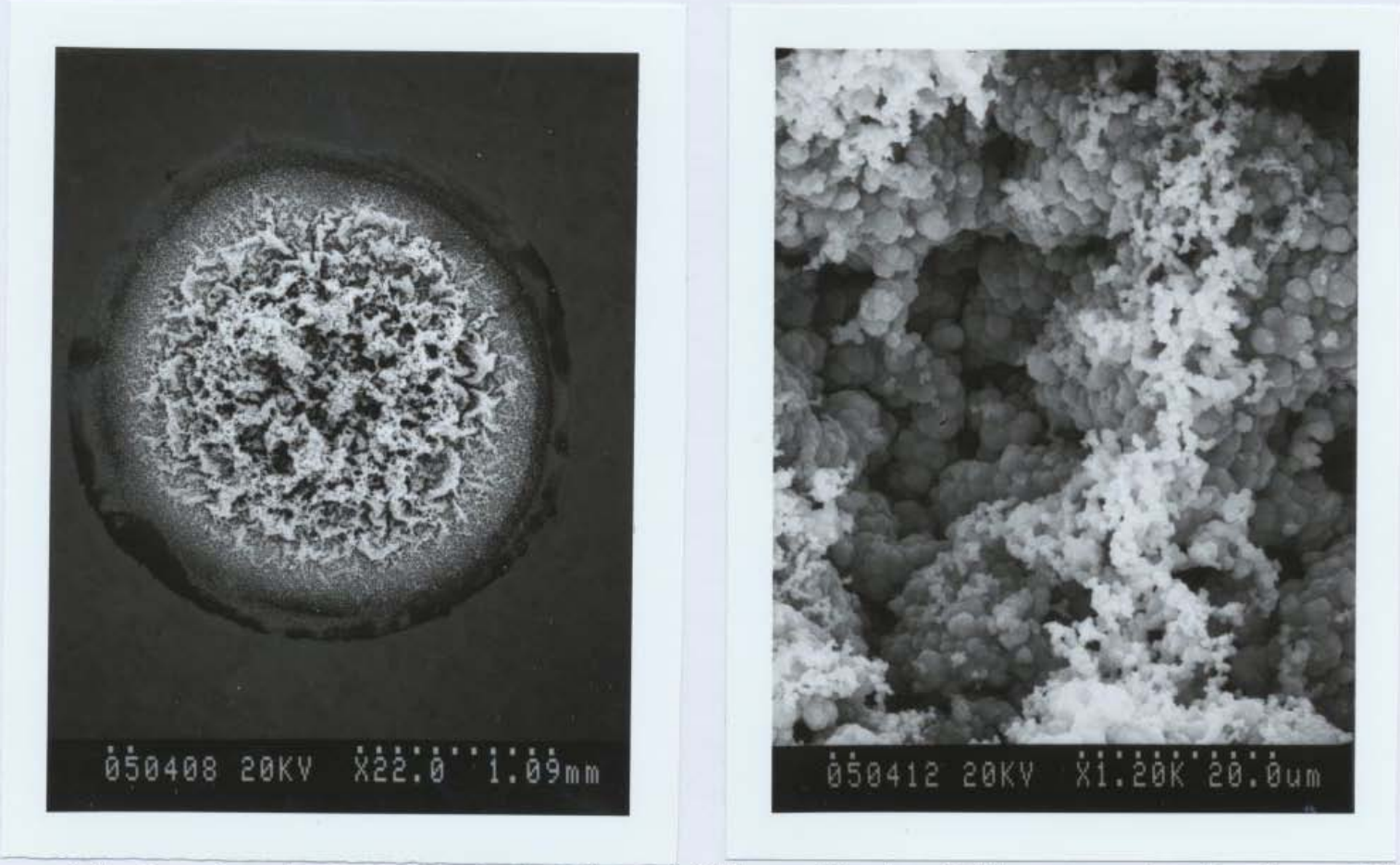

Figure 4.5 Scanning electron micrographs of a poly(3-bromothiophene) film prepared under the conditions specified in Figure 4.2c. The area of the film was 0.0314 cm^2, while the electrode area was only 0.0071 cm^2. The thickness of the film was ca. 100 μm.

When the polymerization process was carried on longer (> ca. 40 scans at higher oxidation potential), streams of brown species were observed diffusing into the bulk solution, presumably as a result of the formation of soluble degradation products with low molecular weight, as in the polymerization of thiophene.[4,23] The loss of soluble products was also observed in cathodic charge vs. scan number plots recorded during the polymerization, as a deviation from the linear increase of cathodic charge at high scan numbers. For this reason, at high upper potential limits, only data for scan numbers up to ca. 30 scans were used to estimate polymerization rates, as was done in Figure 4.2.

4.2.3 Electrochemistry of Polymers

Figure 4.6b shows representative cyclic voltammograms of a poly(3-bromothiophene) film prepared in the presence of bithiophene under the experimental conditions illustrated in Figure 4.2c, recorded in a monomer-free 0.1 M Bu_4NPF_6/acetonitrile electrolyte solution at various scan rates. These curves are quite similar in appearance to those obtained for poly(3-bromothiophene) prepared in the absence of bithiophene (Fig. 4.6a), indicating that the two polymers are essentially the same. In both cases, the major redox process of the polymer is

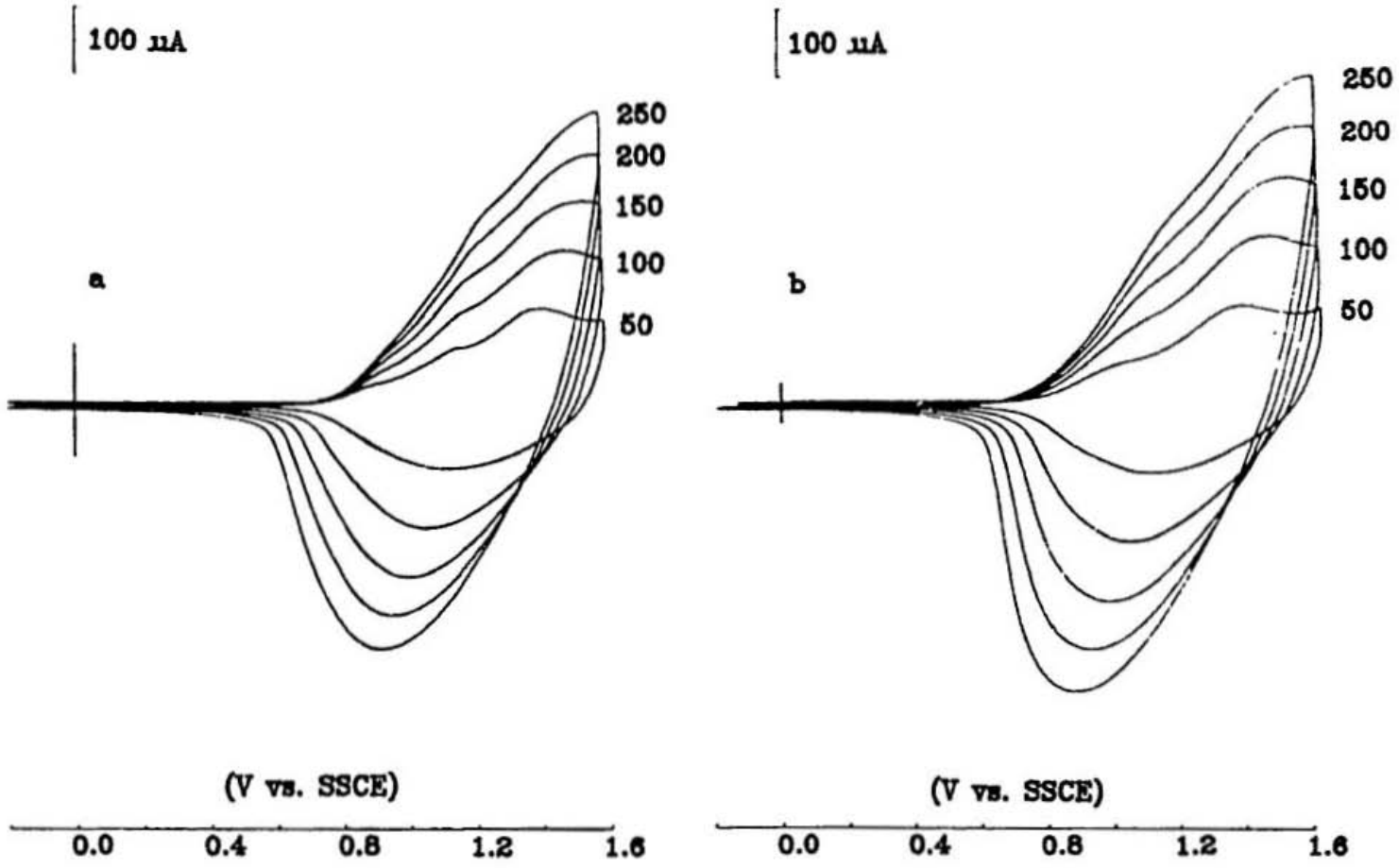

Figure 4.6 Cyclic voltammograms of poly(3-bromothiophene) prepared (a) in the absence and (b) in the presence of 2,2'-bithiophene in 0.1 M Bu_4NPF_6/CH_3CN at various scan rates (mV/s).

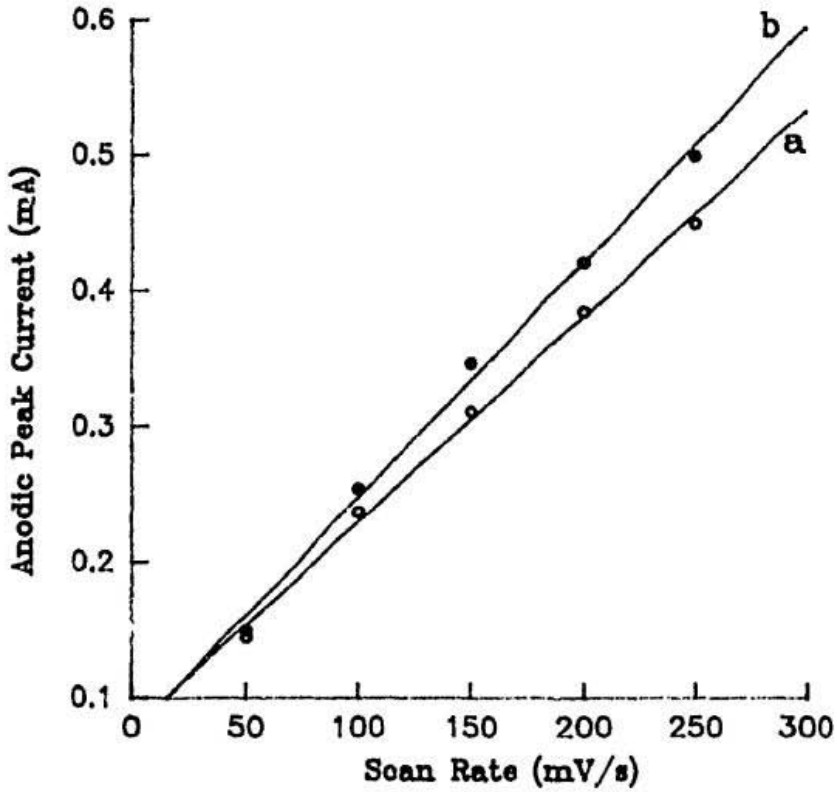

Figure 4.7 Dependence of anodic peak current on scan rate. Data obtained from Figure 4.6, for poly(3-bromothiophene) prepared (a) in the absence and (b) in the presence of 2,2'-bithiophene.

electrochemically reversible,[19] and a linear relationship between anodic peak current (i_{pa}) and scan rate (v) is obtained over the range of 50-250 mV/s (Fig. 4.7), as expected for an electroactive polymer film in the absence of diffusion control.[19,22]

4.2.4 X-Ray Emission Spectroscopy Microanalysis

The insolubility of conducting polymers makes characterization by conventional methods such as IR and NMR difficult. Moreover, it is difficult to obtain reliable elemental analyses of the small samples generated in typical electroanalytical studies. It is therefore not surprising that x-ray emission spectroscopy (XES) has been applied to electrochemically prepared polymer films, because of its advantages over conventional elemental analysis of widespread availability and minimal sample preparation requirements. It has been found that it can provide bulk analysis of thin polymer films up to ca. 5 μm thick.[24]

In contrast to x-ray photoelectron spectroscopy (XPS) which has been applied in a great variety of scientific and technical fields.[25-28] XES has so far been left unexploited in polymer structure analysis, partially because its advantages are offset by the difficulties in quantifying light elements and obtaining information

about chemical environment. However, it has attracted considerable attention in some recent studies on conductive polymers.[24,29,34] Since it is found to be a convenient and useful analytical technique for determining the sulfur and bromine atoms present in the films, we have employed XES here to investigate polymer compositions. In the present investigation, XES spectra of poly(3-bromothiophene) films prepared in the presence of bithiophene are compared with those obtained from bithiophene-free solutions, generated as in Figure 4.2c and 4.2b, respectively.

A typical x-ray spectrum of a poly(3-bromothiophene) film produced in the absence of bithiophene is shown in Figure 4.8a. The polymer coated electrode was removed from the polymerization solution at 0 V immediately after electrochemical synthesis, and thoroughly rinsed with acetone. For analysis by XES, the polymer film was peeled off the electrode surface to prevent any interference from the electrode substrate. Characteristic Br and S peaks appear in the spectrum. In some case, a very small P peak was observed between the Br and S peaks. However, in most cases P was not detected, indicating that most of the electrolyte had been expelled from the polymer film by reduction and rinsing. Energies of x-rays for other elements are too low to be detected under the applied experimental conditions. From the intensities of the Br and S peaks, the relative atomic

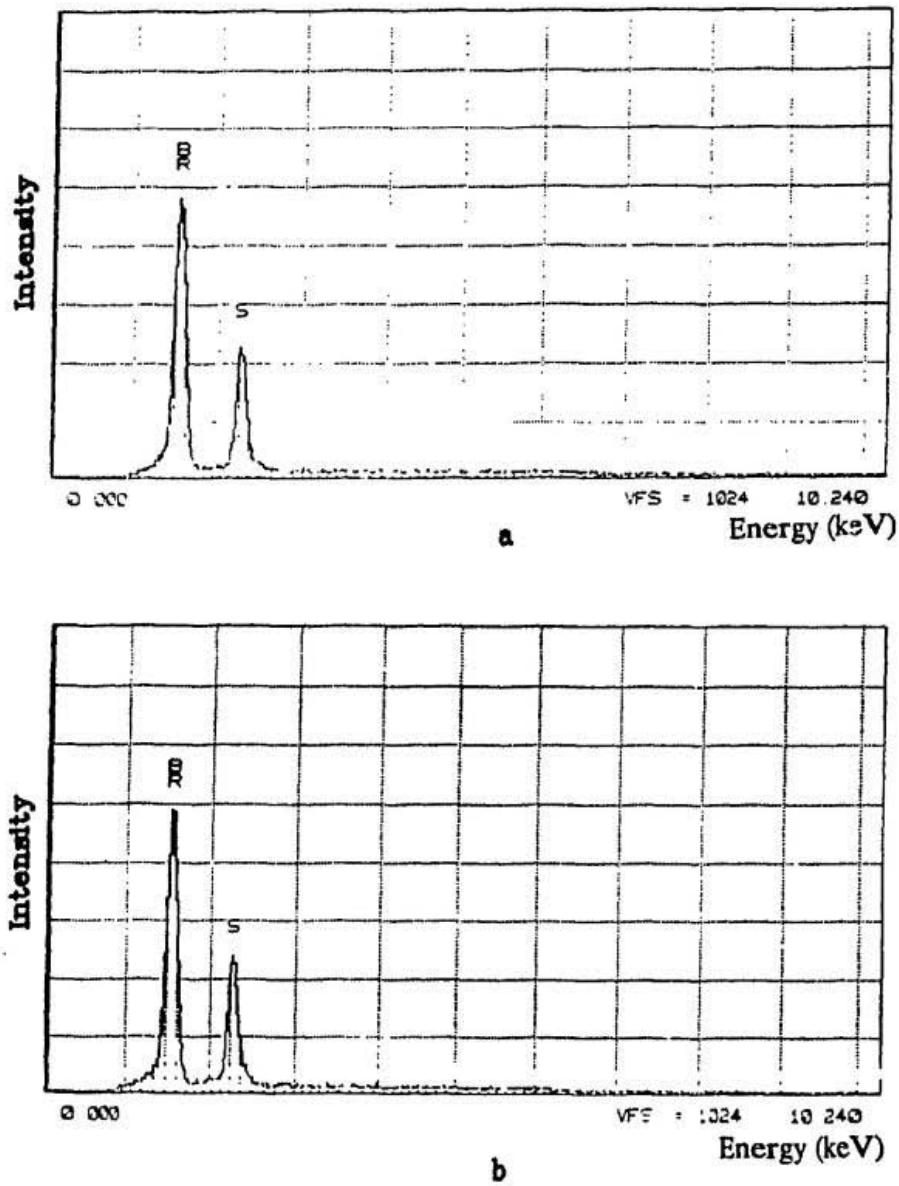

Figure 4.8 X-ray emission spectra of poly(3-bromothiophene) prepared (a) in the absence and (b) in the presence of 2,2'-bithiophene under the condition specified in Figure 4.2.

concentrations of Br and S in the polymer film were estimated using the SQ data analysis program (Section 2.4.2). The atomic concentration ratio of Br:S was calculated as 0.51 for the reduced poly(3-bromothiophene) film. The polymer must have a Br:S ratio of 1:1 for 3-bromothiophene, so apparently the SQ program does not properly correct for the different sensitivities to Br and S. Thus, in our experiments, x-ray emission analysis is about 50% less sensitive to Br than to S, and a factor of 1.96 must be applied to correct the measured Br:S ratio.

For comparison, an X-ray spectrum of poly(3-bromothiophene) generated under the same experimental conditions, but in the presence of a small amount of bithiophene, is given in Figure 4.8b. This spectrum is very similar to that presented above (Fig. 4.8a). The atomic Br:S ratio is 0.50, surprisingly close to the value for pure poly(3-bromothiophene).

Average Br:S ratios for polymers prepared with and without bithiophene using potential cycling to various upper potential limits are listed in Table 4.1. No significant differences are revealed in the data. In fact, the differences among these values are within the experimental error. The results of two sets of data obtained at 1.90 V were compared by using a Student *t* test. The pooled standard deviation

Table 4.1 Average atomic Br:S ratios (uncorrected) determined by XES for poly(3-bromothiophene) films prepared under various conditions

Upper Potential Limit (V vs. SSCE)	In the Absence of BiTh		In the Presence of BiTh	
	Atomic Ratio (Br:S)	No. of Samples	Atomic Ratio (Br:S)	No. of Samples
1.95	0.50 ± 0.004	2	0.50	1
1.90	0.52 ± 0.012	6	0.51 ± 0.030	8
1.85	-	-	0.50 ± 0.023	2
1.80	-	-	0.52	1

s was calculated as 0.024. When the difference of the average for the two sets of data is 0.01, Student's *t* is given as 0.77. Comparing the calculated *t* with the corresponding tabulated *t* (12 degrees of freedom was used) provides that the two results are significantly different at a confidence level of 50%. As a result, a difference of the average of 0.02 would be 80-90% significant, and a difference of the average of 0.03 would be over 95% significant. From the above calculations, 5% thiophene (*i.e.*, 2.5% bithiophene) in poly(3-bromothiophene) films prepared from the mixed solutions could therefore be detected by the XES method. Obviously, none of the data presented in Table 4.1 suggests the presence of bithiophene units in the resulting polymer films. Hence, it appears that reasonably pure poly(3-bromothiophene) is produced in the presence of bithiophene, even at potentials as low as 1.8 V (Table 4.1).

In summary, the small amount of 2,2'-bithiophene added into the solution does not co-polymerize with the bromothiophene, but rather catalyzes the polymerization of the latter. This agrees with Wei et al.'s[10] conclusion for the methylthiophene/bithiophene system which was based on IR spectroscopy. IR spectroscopic studies usually require a larger sample amount (*e.g.*, 2-5 mg for solid sample detection) than XES, which means a long polymerization process is

required. In the case of bromothiophene, this will lead to polymer degradation. For other very thin polymers with strong adherence on the electrode, it is very difficult to carry out IR spectroscopic analysis. In contrast, XES has been easily applied to such samples.

4.3 Discussion

A key result emerging from the electrochemical polymerization data (*i.e.*, cyclic voltammograms and plots of cathodic charge vs. scan number) and characterization of polymer films (*i.e.*, morphological, electrochemical and x-ray emission spectroscopic studies) is that more rapid poly(3-bromothiophene) growth can be achieved by introducing a small amount of bithiophene into the bromothiophene solution. That is, 2,2'-bithiophene can facilitate the polymerization of 3-bromothiophene, as well as that of polythiophene and poly(3-alkylthiophene)s as previously reported.[9]

Since the oxidation of bithiophene takes place at a lower potential than for bromothiophene,[4] the bithiophene in the polymerization system is oxidized first

(Fig. 4.1b), producing nucleating species that may induce the polymerization of bromothiophene at a lower potential than normal. Therefore, in the presence of bithiophene, the number of nucleation sites is greater than in the absence of bithiophene, resulting in more oligomeric and polymeric species in each individual scan and thus a higher overall rate of polymerization.

As in the studies of poly(3-methylthiophene) under potentiostatic conditions (Section 3.2.1), an induction period appears in plots of cathodic charge vs. scan number for the early stages of polymerization of 3-bromothiophene (Fig. 4.2). This induction period is also related to the formation of nuclei on the Pt electrode or in the solution near the electrode surface. In the early stages of the polymerization, the number of nucleation sites increases during each cycle, as do the amount of oligomer and polymer on the electrode. With the addition of bithiophene, the number of the nuclei in the polymerization system increases and this shortens the induction time.

4.4 Conclusions

It has been shown that a small amount of bithiophene can significantly improve the electrochemical polymerization of bromothiophene. It can not only effectively shorten the initial induction period and lower the required upper potential limit, but also enhance the overall polymerization rate. Side reactions such as mislinkage and degradation of polymer will be minimized, since a lower oxidation potential can be applied.

Polymer films prepared in the presence of bithiophene have been characterized by cyclic voltammetry, scanning electron microscopy and x-ray emission spectroscopy, and have been compared with poly(3-bromothiophene) films generated in the absence of bithiophene. Neither differences in composition, morphology nor electrochemical properties were detected. It appears that the amount of bithiophene incorporated into the poly(3-bromothiophene) films, if any, is insignificant under the chosen conditions.

As a conclusion, a fast electrochemical polymerization of bromothiophene can be achieved by introducing a catalytic amount of bithiophene into the

poly.nerization system. The results are in good agreement with those reported in the literature for the thiophene/bithiophene and 3-alkylthiophene/bithiophene systems. The kinetics and mechanism of the polymerization are discussed in the following chapter.

References

1. M. Lemaire, D. Delabouglise, R. Garreau, A. Guy, and J. Roncali, *J. Chem. Soc., Chem. Commun.*, 1988, **9**, 658.

2. D. Kottar, V. Joshi, and P.K. Ghosh, *J. Chem. Soc., Chem. Commun.*, 1988, **14**, 917.

3. J. Roncali, R. Garreau, D. Delabouglise, F. Garnier, and M. Lemaire, *Synth. Met.*, 1989, **28**, C341.

4. R.J. Waltman, J. Bargon, and A.F. Diaz, *J. Phys. Chem.*, 1983, **87**, 1459.

5. L.H. Shi, J. Roncali, and F. Garnier, *J. Electroanal. Chem.*, 1989, **263**, 155.

6. T.L. Porter, S. Jeffers, G. Caple, B.L. Wheeler, and R. Swift, *Surf. Sci.*, 1990, **238**, 433.

7. G. Caple, B.L. Wheeler, T.L. Porter, and S. Jeffers, *J. Phys. Chem.*, 1990, **94**, 5639.

8. J. Roncali, R. Garreau, A. Yassar, P. Marque, F. Garnier, and M. Lemaire, *J. Phys. Chem.*, 1987, **91**, 6706.

9. Y. Wei, C.-C. Chan, J. Tian, G.-W. Jang, and K.F. Hsueh, *Chem. Mater.*, 1991, **3**, 888.

10. Y. Wei, G.-W. Jang, and C.-C. Chan, *J. Polym. Sci., Part C: Polym. Lett.*, 1990, **28**, 219.

11. Y. Wei, G.-W. Jang, C.-C. Chan, K.F. Hsueh, R. Hariharan, S.A. Patel, and C.K. Whitecar, *J. Phys. Chem.*, 1990, **94**, 7716.

12. B. Krische and M. Zagorska, *Synth. Met.*, 1989, **28**, C263.

13. P. Marque, J. Roncali, and F. Garnier, *J. Electroanal. Chem.*, 1987, **218**, 107.

14. A.F. Diaz, J. Crowley, J. Bargon, G.P. Gardini, and J.B. Torrance, *J. Electroanal. Chem.*, 1981, **121**, 355.

15. L. Laguren-Davidson, C.V. Pham, H. Zimmer, H.B. Mark Jr., and D.J. Ondrus, *J. Electrochem. Soc.*, 1988, **135**, 1406.

16. S. Asavapiriyanont, G.K. Chandler, G.A. Gunawardena, and D. Pletcher, *J. Electroanal. Chem.*, 1984, **177**, 229.

17. J.P. Ferraris and T.R. Hanlon, *Polymer*, 1989, **30**, 1319.

18. A. Yassar, J. Roncali, and F. Garnier, *Macromolecules*, 1989, **22**, 804.

19. G. Tourillon, in *Handbook of Conducting Polymers*, vol. 1, T.A. Skotheim, Ed. (Marcel Dekker, New York, 1986), pp. 293-350.

20. F. Beck, P. Braun, and M. Oberst, *Ber. Bunsenges. Phys. Chem.*, 1987, **91**, 967.

21. F. Beck, P. Braun, and Schloten, *J. Electroanal. Chem.*, 1989, **267**, 141.

22. E.W. Tsai, S. Basak, J.P. Ruiz, J.R. Reynolds, and K. Rajeshwar, *J. Electrochem. Soc.*, 1989, **136**, 3683.

23. M.R. Bryce, A.D. Chissel, N.R.M. Smith, D. Karker, and P. Kathirgamanathan, *Synth. Met.*, 1988, **26**, 153.

24. Z. Qi and P.G. Pickup, *Anal. Chem.*, 1993, **65**, 696.

25. H.D. Abruna, P. Denisevich, M. Umana, T.J. Meyer, and R.W. Murray, *J. Am. Chem. Soc.*, 1981, **103**, 1.

26. W.R. Salaneck, R. Erlandsson, J. Prejza, I. Lundstrom, and O. Inganas, *Synth. Met.*, 1983, **5**, 125.

27. J.C. Scott, J.L. Bredas, K. Yakushi, P. Pfluger, and G.B. Street, *Synth. Met.*, 1984, **9**, 165.

28. W. Torres and M.A. Fox, *Chem. Mater.*, 1992, **4**, 146.

29. G.L. Duffitt and P.G. Pickup, *J. Chem. Soc., Faraday. Trans.*, 1992, **88**, 1417.

30. S. Dong and G. Lian, *J. Electroanal. Chem.*, 1990, **291**, 23.

31. T. Iyoda, H. Toyoda, M. Fujitsuka, R. Nakahara, H. Tsuchiya, K. Honda, and T. Shimidzu, *J. Phys. Chem.*, 1991, **95**, 5215.

32. P. Boulanger, C. Magermans, J.J. Verbist, J. Delhalle, and D.S. Urch, *Macromolecules*, 1991, **24**, 2757.

33. S. Kuwabata, K. Okamoto, and H. Yoneyama, *J. Chem. Soc., Faraday. Trans. I*, 1988, **84**, 2317.

34. J. Ochmanska and P.G. Pickup, *Can. J. Chem.*, 1991, **69**, 653.

Chapter 5

Kinetics and Mechanism of Electropolymerization of 3-Bromothiophene in the Presence of 2,2'-Bithiophene

5.1 Introduction

Since the kinetics of polymer formation in the presence of additives leads to a further understanding of the mechanism, investigations have been done on the 3-methylthiophene/bithiophene and other systems.[1] A mechanism has been proposed by Wei's group for the polymerization of thiophene and 3-alkylthiophenes, based on the experimental observations obtained in the presence of additives.[1] This mechanism involves a radical attack on a neutral monomer for the polymeric chain propagation, in contrast to the more accepted radical-coupling mechanism (Section 1.2.1) where the coupling of two radicals leads to successive electrochemical and chemical processes of electropolymerization.

The overall rate of polymer formation is affected by several variables

including the monomer concentration,[2,3] the concentration[4] and nature[5] of the counterion as well as the applied potential, size of the electrode, *etc*. The purpose of our study was to determine the effects of the concentrations of 3-bromothiophene monomer ($[M]$) and of 2,2'-bithiophene catalyst ($[C]$) on the rate of polymerization. The experiments were carried out in bromothiophene/bithiophene solutions.

5.2 Results

As reported in Section 4.2.1, the charge for reduction of poly(3-bromothiophene) deposited on the electrode was measured for successive scans during potential cyclic polymerization. The linear relationship between the cathodic charge (Q_c) and the scan number (s) (*i.e.*, the reaction time t) after the initial stages of nucleation and growth indicates that the increase of the amount of poly(3-bromothiophene) on the electrode is the same for each consecutive scan and the defined rate of polymerization (dQ_c/ds) is constant, which provides us with a useful and convenient method to determine the rate of steady polymerization.

To minimize the effects of water on the polymerization rate, in this chapter, acetonitrile containing ca. 0.1% water by weight was used as the solvent, in contrast to that containing 0.3% water by weight used in the previous chapter. All other experimental procedures were the same as in Chapter 4.

5.2.1 Dependence of the Rate of Polymerization on Monomer Concentration

Plots of cathodic charges (which is proportional to the amount of polymer) as a function of scan number and the reaction time measured at different concentrations of the bromothiophene monomer in the range of 0.05 to 0.3 M are shown in Figure 5.1. The concentration of bithiophene was kept constant at 0.2 mM. The polymer grows at an increasing rate as the monomer concentration is increased. For each individual plot, it is apparent that the cathodic charge is directly proportional to the scan number after the induction period.

The rates of steady polymer formation were measured from the linear parts of the plots in Figure 5.1, by discarding the data points in the initial induction period. A plot of the polymerization rate vs. the monomer concentration is shown in Figure 5.2. The higher the concentration of bromothiophene, the faster the rate

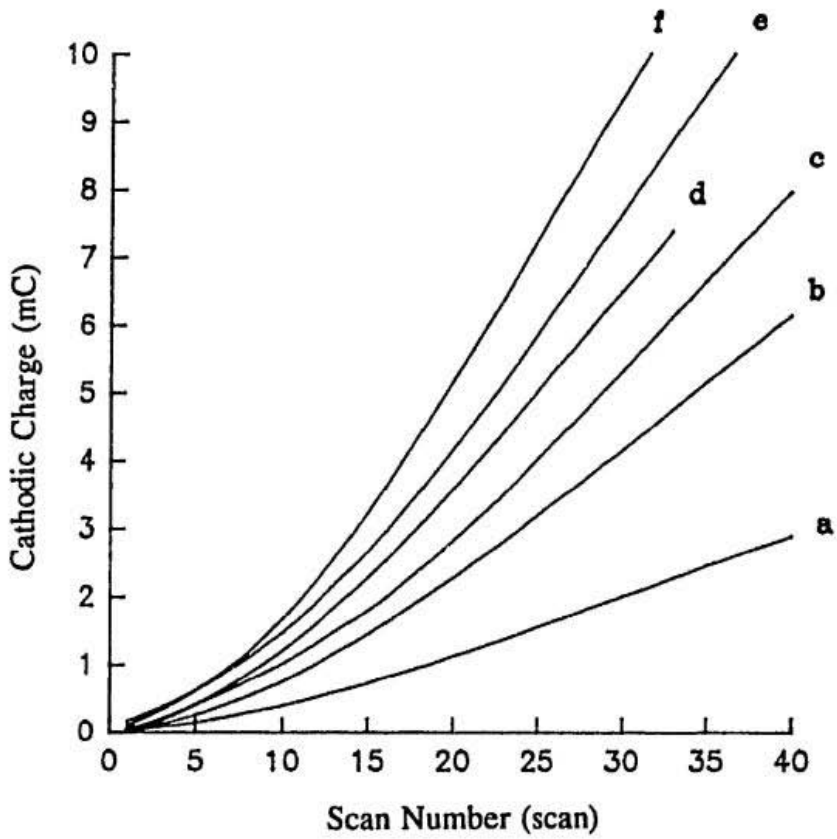

Figure 5.1 Plots of the cathodic charge against the scan number for the polymerization of 3-bromothiophene at concentrations of (a) 0.05; (b) 0.10; (c) 0.15; (d) 0.20; (e) 0.25 and (f) 0.30 M in the presence of 0.2 mM 2,2'-bithiophene. Potential cycling range: -0.2 to 1.9 V. Scan rate: 50 mV/s.

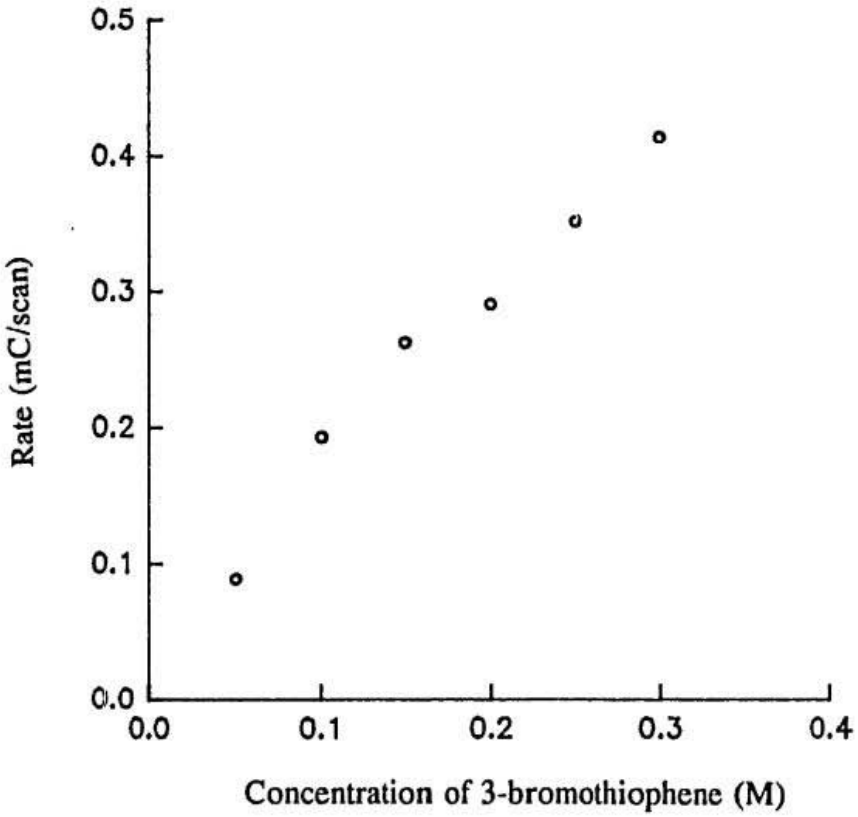

Figure 5.2 The polymerization rates (*i.e.*, the slopes from Figure 5.1) at various concentrations of 3-bromothiophene.

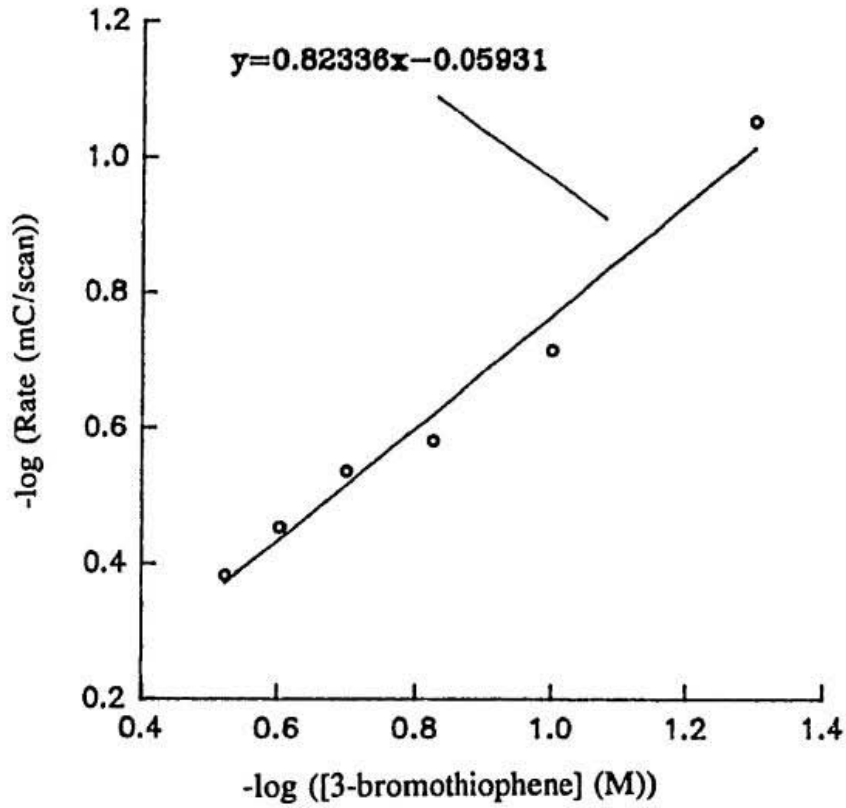

Figure 5.3 Relationship between the polymerization rate (*i.e.*, the slopes from Figure 5.1) and the concentration of 3-bromothiophene.

of polymer generation. A slope of 0.82 measured from a plot of log (dQ_c/ds) vs. log $/M/$ (Fig. 5.3) indicates that the defined rate of polymerization (R) is approximately first order with respect to the bromothiophene concentration ($/M/$) in the concentration range investigated, as expressed in Equation 5.1,

$$R = k^{app'}/M/ \qquad \text{(Eq. 5.1)}$$

where $k^{app'}=k^{app}/C/^x$. k^{app} is an apparent rate constant, and x represents the extent of dependence of rate on the bithiophene concentration ($/C/$).

5.2.2 Effects of Bithiophene Concentration on the Rate of Polymerization

To investigate the influence of a catalytic amount of bithiophene on the polymerization rate, studies have been done by changing the concentration of bithiophene in the range of 0.05 to 0.5 mM, whereas 0.2 M bromothiophene was used in each case. Figure 5.4 shows plots of cathodic charge against scan number recorded during the polymerization at various concentrations of bithiophene. In general, the polymer grows faster when the concentration of bithiophene becomes higher. In each individual plot, the cathodic charge increases proportionally to the scan number after induction period. As demonstrated in Figure 5.5, a plot of log (dQ_c/ds) (*i.e.*, the slopes from plots in Figure 5.4) vs. log $/C/$ gives a linear line

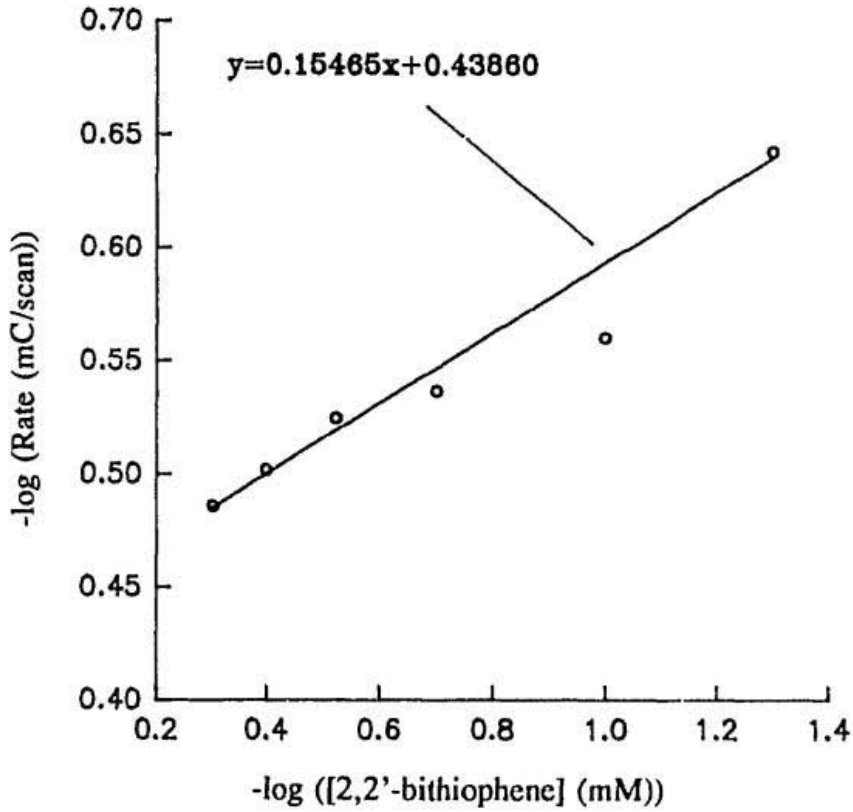

Figure 5.5 Relationship between the polymerization rate (*i.e.*, the slopes from Figure 5.4) and the concentration of 2,2'-bithiophene.

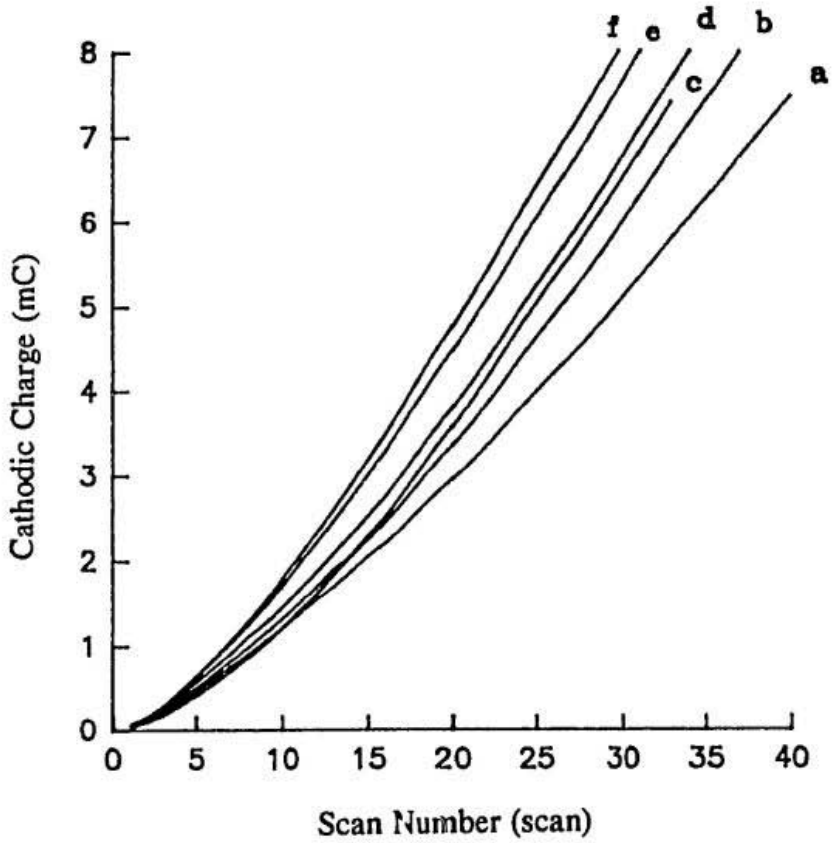

Figure 5.4 Plots of the cathodic charge against the scan number for the polymerization of 0.2 M 3-bromothiophene in the presence of 2,2'-bithiophene at concentrations of (a) 0.05; (b) 0.10; (c) 0.20; (d) 0.30; (e) 0.40 and (f) 0.50 mM in the potential cycling range of -0.2 to 1.9 V. Scan rate: 50 mV/s.

with a slope of 0.15, indicating that the rate of polymerization is approximately 0.15 order with respect to the bithiophene concentration in the solution of constant bromothiophene concentration. Thus the empirical rate can be expressed as

$$R = k^{app''}[C]^{0.15} \qquad \text{(Eq. 5.2)}$$

where $k^{app''} = k^{app}[M]$.

Combining Equation 5.1 with Equation 5.2, a general empirical rate expression of the polymerization of bromothiophene in the presence of a small amount of bithiophene can be derived and written as

$$R = k^{app}[M][C]^{0.15} \qquad \text{(Eq. 5.3)}$$

5.2.3 Effects of Water on the Polymerization Rate

It was suggested that the presence of water in the polymerization solution has deleterious consequences for the electropolymerization reaction[6,7] This was also observed in our experiments. As mentioned before, a synthesis medium containing a comparatively large amount of water (*i.e.*, ca. 0.13 M) was used in Chapter 4, while solutions with lower water concentrations (ca. 0.04 M) were used in the kinetic studies. It is clear that the polymerization rate decreases with increasing the

water content. For example, comparing Figure 5.1d with Figure 4.2c, although both polymerizations were carried out under the same conditions except that the experiments of the former contained less water in the solution, the polymerization rate for the lower water-content polymerization was 69% higher. However, the water content did not change the catalytic behaviour of bithiophene, because an increase of 30-35% in the polymerization rate was observed in both sets of polymerization, regardless of the amount of water in the solution.

The reason for the inhibitory effect of water is not fully understood. We speculated that it acts as a nucleophile to react with the monomeric and oligomeric radical cations or the growing polymer chain ends.

5.3 Discussion

The experimental results reported in the previous and present chapters are to some degree consistent with Wei's work.[1] In some aspects, the conventional radical-coupling mechanism has difficulties in interpreting the experimental observations concerning the decrease of applied oxidation potential, and the

enhancement of overall polymerization rate in the presence of 2,2'-bithiophene. At low oxidation potentials, the radical-radical coupling would have taken place between bithiophene radicals, since although some bromothiophene radicals were expected to be present, the concentration of bithiophene radical is relatively higher under the potential applied. The polymer films prepared at low potentials would be therefore similar to poly(2,2'-bithiophene) which is contrary to cyclic voltammetry and XES analysis of the resulting polymer films. In addition, according to the radical-radical coupling mechanism, a certain overpotential must be applied to maintain an essential amount of monomeric radical cation as the polymerization proceeds. It thus can not explain the polymerization of 3-bromothiophene at a lower potential than normal.

The alternative radical-monomer coupling mechanism (Section 1.2.2) is therefore applied to rationalize the experimental data, similar to that proposed by Wei's group.[1] The first step, that is the oxidation of monomer to form a radical cation, has been demonstrated to be the rate-determining step in the polymerization of 3-methylthiophene.[1] However, in our studies with bromothiophene, this slow step was intentionally avoided by introducing a catalytic amount of 2,2'-bithiophene which has a lower oxidation potential into the polymerization system, resulting in

a substantial enhancement of the overall rate of polymerization. Since bithiophene is oxidized first, it provides electroactive radical cations that readily react with the nucleophilic bromothiophene monomer at a relatively low oxidation potential, and then contribute to the polymer growth.

Mechanisms of Poly(3-bromothiophene) Deposition in the Presence of Bithiophene

Although the mechanism of the rate enhancement effects of bithiophene on the polymerization of bromothiophene is far from a full understanding, the mechanisms shown in Schemes 5.1 and 5.2 appear most plausible. In both schemes, the first step is assumed to be the oxidation of bithiophene since this occurs at much lower potential than oxidation of the bromothiophene monomer.

In Scheme 5.1, the bithiophene radical cation formed in the first step oxidizes the bromothiophene monomer and returns to the neutral state to be oxidized again. The bromothiophene cation generated then reacts with a neutral monomer to produce a dimer, after loss of two protons and an electron as in Scheme 5.1. Since the oxidation of the dimer and successive oligomers occurs at

SCHEME 5.1

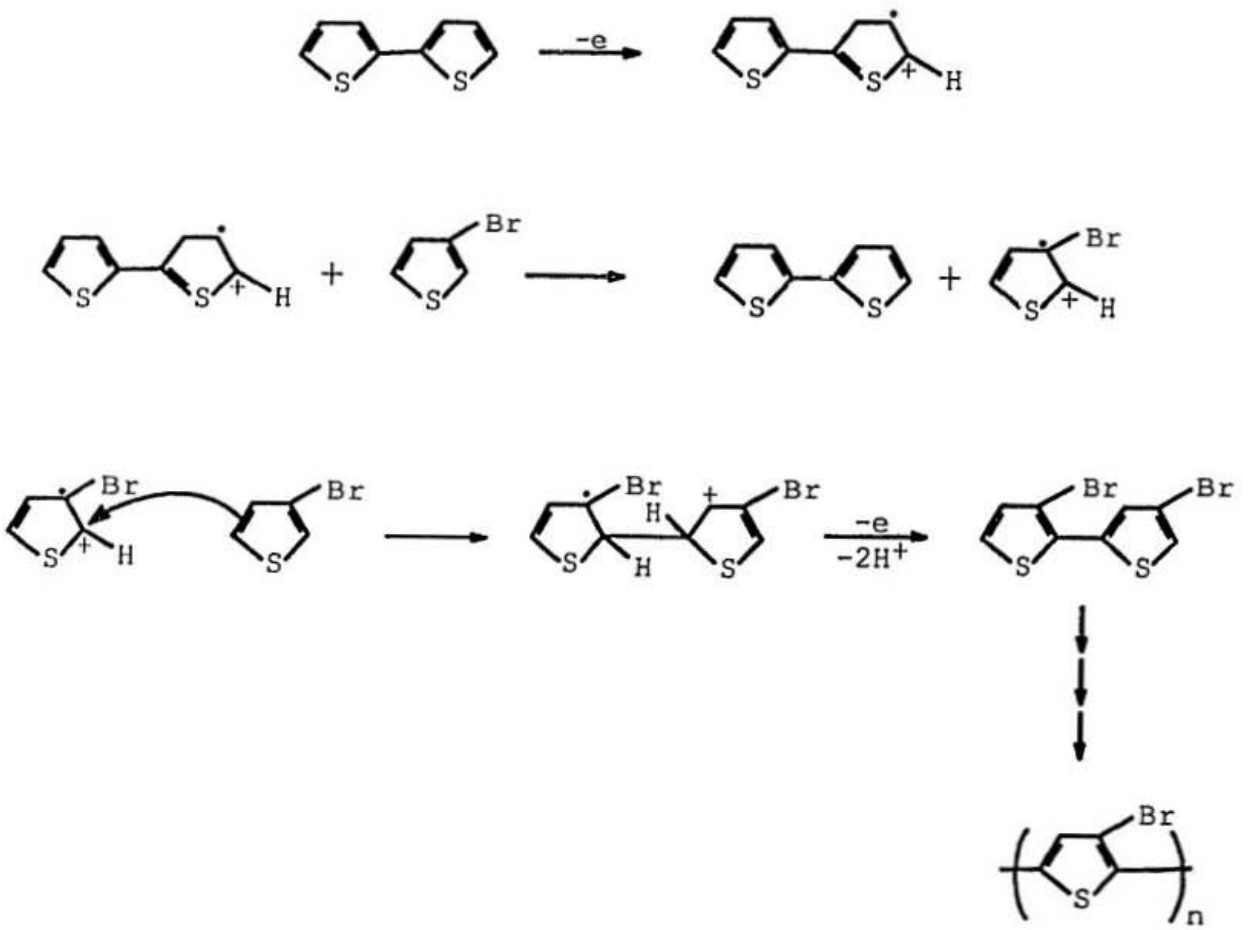

SCHEME 5.2

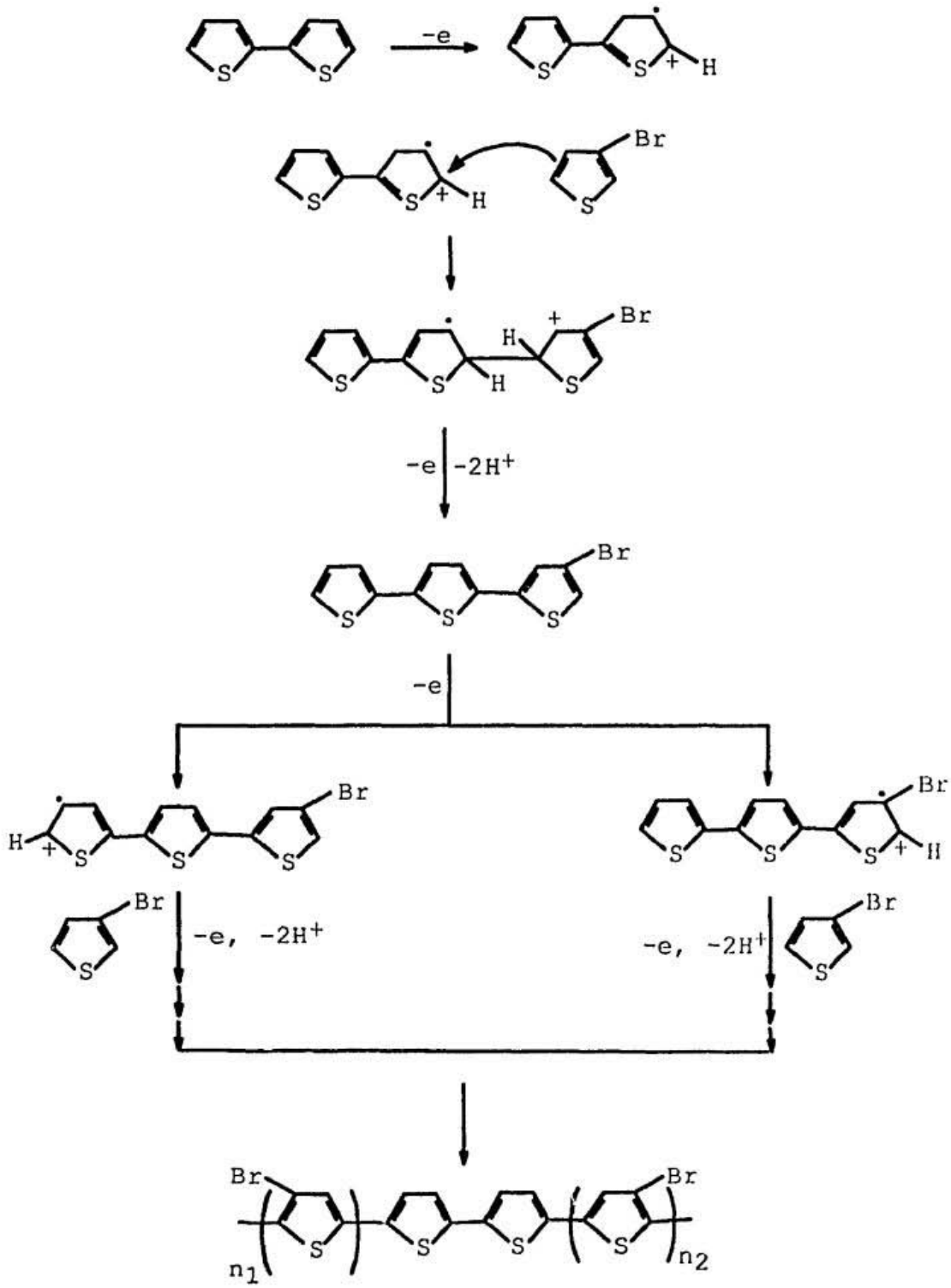

lower potentials, they undergo further electrochemical oxidation and couple with monomeric bromothiophene. Through these successive electrochemical and chemical steps, oligomers and polymers deposit on the electrode surface when they are large enough to be insoluble. In this scheme, the bithiophene in the system acts as a catalyst in the true sense; catalyzing the oxidation of bromothiophene at a lower overpotential and at higher reaction rate, but not being incorporated into the polymer chains. The most significant role of the bithiophene is presumably initiation of the polymerization as shown in Scheme 5.1. It may also catalyze the oxidation of intermediates.

The bithiophene could also function as an initiator by coupling with bromothiophene as outlined in Scheme 5.2. After the generation of a bithiophene radical cation, it is postulated that the radical cation could react with a bromothiophene monomer to produce a bromothiophene-bithiophene trimer after further deprotonation and oxidation, instead of producing a bromothiophene cation only as in Scheme 5.1. This trimer would be further oxidized and couple with a bromothiophene monomer due to the much higher concentration of bromothiophene in the solution. Oligomers and polymers would be produced as discussed before and eventually deposit on the electrode. This mechanism produces a polymer

containing bithiophene, but since only a small amount of bithiophene is added to the polymerization system, it will be present in the polymer film in such a small amount that its effects on the structure of the resulting polymer will be minimal. This mechanism is therefore consistent with electrochemical and spectroscopic results discussed in Chapter 4.

Although the polymerization is unlikely to occur solely through the direct oxidation of bromothiophene monomer, the radical-radical coupling of monomeric radical cations may also take place, since some bromothiophene radical cations may still be produced under the potential applied. However, as discussed in the previous subsection, this polymerization process can not fully account for the polymer growth with a faster polymerization rate and at lower oxidation potential, as well as for the cyclic voltammetry and XES studies of the resulting polymers.

5.4 Conclusions

The influence of both bromothiophene monomer and bithiophene additive concentrations on the overall rate of electropolymerization of bromothiophene has

been investigated. It is shown that the rate of polymer formation is approximately first order with respect to bromothiophene monomer concentration and ca. 0.15 order with respect to the bithiophene catalyst concentration. Although the electrolyte medium contained less water in these experiments, the extent of rate enhancement was comparable to that presented in Chapter 4. That is, regardless of the amount of water in the medium, the polymerization rate in the presence of bithiophene is 30-35% higher than that in the absence of bithiophene. However, as a whole, the rate of polymer formation decreases with the increase of water concentration in the synthesis medium.

Tentative mechanisms for the electrochemical polymerization of poly(3-bromothiophene) in the absence and presence of bithiophene have been proposed. Some mechanisms have been proposed to account for the experimental observations, where bithiophene in the mixed solution may function either as an electron acceptor or as an initiator as demonstrated in Scheme 5.1 and 5.2, respectively.

References

1. Y. Wei, C.-C. Chan, J. Tian, G.-W. Jang, and K.F. Hsueh, *Chem. Mater.*, 1991, **3**, 888.

2. R. John and G.G. Wallace, *Polymer International*, 1992, **27**, 255.

3. B. Krische and M. Zagorska, *Synth. Met.*, 1989, **33**, 257.

4. S. Kuwabata, K. Okamoto, and H. Yoneyama, *J. Chem. Soc., Faraday. Trans. I*, 1988, **84**, 2317.

5. G. Tourillon and F. Garnier, *J. Pol. Sci., Part A, Pol. Chem.*, 1984, **22**, 33.

6. A.J. Downard and D. Pletcher, *J. Electroanal. Chem.*, 1986, **206**, 147.

7. A.R. Hillman and E. Mallen, *J. Electroanal. Chem.*, 1988, **243**, 403.